J-like aggregation of a cationic polythiophene with hydrogen-bonding capabilities due to 1,4-dioxane: solution excitation spectra and fluorescence, morphology and surface free energy of films

Sergio E. Domínguez*†, Antti Vuolle†, Ciarán Butler-Hallissey‡, Timo Ääritalo†, Pia Damlin† and Carita Kvarnström†

†*Department of Chemistry, Turku University Centre for Materials and Surfaces (MATSURF), University of Turku, 20014 Turku, Finland*

‡*Turku Bioscience Centre, University of Turku and Åbo Akademi University, Turku, Finland*

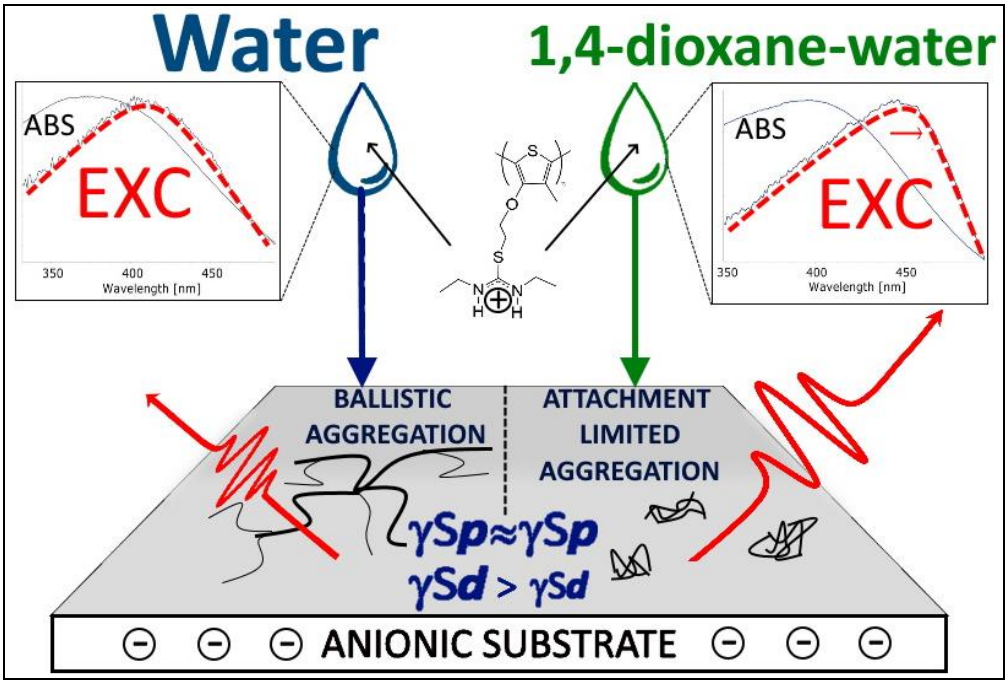

ABSTRACT

This work presents solution- and solid-state evidence of the enhancement of J-like aggregation of a cationic polythiophene (CPT) with isothiouronium functionalities (PT1), caused by a decrease in the polarity and hydrogen-bonding (H-bonding) capacity of the solvent, generated by using a 50:50 v/v 1,4-dioxane-water mixture (W-DI) instead of water. In solution, the presence of 1,4-dioxane (DI) in solution seems to generate selective solvation, tuning the energy transfer within PT1 from inter-chain into intra-chain, enhancing J-like aggregation. On the other hand, during the casting process, the presence of DI directs the interaction with solid-substrates, generating an increase in the solid-state fluorescence, modifying the morphology from one similar to ballistic-aggregation (BA) into one similar to attachment limited aggregation (ALA), also DI modifies the SFE by increasing slightly its polar contribution ($\gamma S\boldsymbol{p}$) and decreasing the dispersive one ($\gamma S\boldsymbol{d}$).These results can be explained to be caused by a "coating" effect in presence of DI (as proposed before experimentally and computationally).

Our results show a clear correlation between the solution- and solid-state properties of PT1 in each solvent, further validating the use of the fluorescence excitation spectra to trace J-like aggregation of water-soluble conjugated polymeric fluorophores in solution. This information could be useful for predicting and designing specific mesoscopic architectures of CPTs (and conjugated polyelectrolytes in general), which are molecules lacking of clear structure-function guidelines for designing high-performance polythiophene-based interlayer materials, especially for CPTs (and conjugated polyelectrolytes (CPEs) in general), particularly those with H-bonding capabilities. To the best of our knowledge the use of solution-state fluorescence excitation spectra to identify J-like aggregation of water-soluble conjugated polymers (CPs) has been scarcely used/discussed in literature and no correlation with solid-state properties was reported previously.

Keywords: conjugated polyelectrolytes, cationic polythiophenes, isothiouronium, charge-assisted Hydrogen-bond, J-like aggregation, UV-Vis, fluorescence spectroscopy, drop-casting, fluorescence microscopy, spin-coating, plasma activated glass, static contact angle, surface free energy, mica, AFM.

INTRODUCTION

Aggregation of pi-conjugated molecules is relevant because the functional properties and the electronic interactions between building blocks can easily be modulated by varying the temperature, solvent polarity, and concentration.[1] Self-assembling molecules can be exploited to generate ordered aggregates, which is relevant for both fundamental and applied research. For example, the performance of organic semiconducting molecules in optoelectronic applications depends on the functional properties of the individual molecules and on their mutual orientations in the solid-state, which can be tuned in solution, during the early stages of aggregation.

Small molecules and polymers have pros and cons in regard to their characterization and applications. Small molecules present smaller variability between batches and are easier to purify and characterize, however, polymers generate larger conjugation lengths. Therefore, small molecules represent a better system to study H- and J-aggregation, while polymeric molecules present better properties for some optoelectronic applications. Indeed, H- and J-aggregates were firstly studied in *dye assemblies*, which often form these aggregates depending on the relative alignment of the transition dipole moments in adjacent molecules. In an H-aggregate, the intramolecular stacking is predominantly face-to-face, while in J-aggregates the stacking is predominantly head-to-tail.[2] J-aggregates were originally exploited in photographic processes or to modulate light signals in optical communication devices.[3] Currently the ultimate goal is tuning the solid-state functional properties of molecules and their mutual orientations.[2] Thus, the study of H-J aggregation contributes to understanding the role of molecular packing and effect on the materials photovoltaic performance. H- and J-aggregation strongly modify the optical absorption and fluorescence features, which has important consequences for the oscillator strengths of the transitions from the ground to the excited states (S0->S1 transitions), and the energies thereof.[2] H-aggregates exhibit blue-shifted absorption spectra in respect to the absorption of the monomer, and are subradiant. On the other hand J-aggregates exhibit the opposite behavior, red-shifted absorption spectra (in respect to the monomer) and are superradiant.[4]

The concept of H-J aggregation was expanded by Spano et al. to analyze films of polythiophenes, in order to perform structure-function studies.[5] Particularly for polythiophenes, H- and J-aggregates coexist in the form of “H-J aggregates”, and the contribution of each mode differs in every practical situation.[5] For structured absorption-fluorescence spectra, the ratio of the first two vibronic peak intensities provides further information, with H(J)-aggregates showing a decrease (increase) in this ratio with increasing excitonic coupling, while the ratio of the 0-0 to 0-1 emission intensities (decreases) with disorder and increases (decreases) with increasing temperature. In absorption and emission spectra, values smaller than 1 in the A1/A2 oscillator strength ratios indicate significant inter-chain coupling (characteristic of H-aggregates) in the aggregates.[4] Indeed, these emission ratios are limiting cases that provide a framework which allow to interpret absorption/emission in more complex morphologies, such as herringbone packing in oligo(phenylene vinylene)s, oligothiophenes and polyacene crystals, as well as the polymorphic packing arrangements observed in carotenoids.[4] Zhu et al.[6] used this concept to study the molecular ordering in solution, of a hydrophilic, thermo-responsive polythiophene, with ethylene oxide side groups, using absorption in solution and synchrotron X-ray scattering to track co-facial stacking (i.e. [010] ordering) and cofacial molecular stacking (i.e. [100] ordering). The well-defined structuring of both absorption and fluorescence allowed comparing the 0−0/0−1 ratio in order to estimate the [010] ordering.

Structured spectra is also generated by nanofibers or thin films, in which case it is possible to gain understanding on the exciton coupling present (i.e. intra- or inter-chain), as shown in previous studies on poly-3-hexylthiophene (P3HT), one of the most studied polymers for organic solar cells applications.[7–9]

Besides absorption and fluorescence spectra, the excitation spectrum also provides information on H-J like aggregation of water-soluble polymers and small molecules. However, to the best of our knowledge, this method has been scarcely reported in literature. Deng et al.,[10] observed that an increase in the concentration in aqueous solutions of lignosulfonates generates a distortion in the fluorescence excitation spectrum, without modifying the fluorescence emission spectrum. In an analogous study, we used the excitation spectra to study the solution concentration-driven aggregation of cationic polythiophenes (CPTs) with hydrogen-bonding (H-bonding) capabilities, as a function of the side-chain length and the polarity and H-bonding capacity of the solvent.[11]

The excitation spectra has shown to be informative on H-J aggregation of small molecules, because it is capable of detecting the spectral response to pi-pi stacking of aromatic groups.[10] This criterion has also been used in studies using small molecules, such as a near-infrared dye, as a function of concentration and solvent.[12]

In the solid-state, the analysis of the morphology and/or fluorescence of films deposited onto mica (using atomic force microscopy (AFM) and fluorescence microscopy), are a useful approaches to study the impact of solvent dependent, solution- and solid-state properties, of cationic molecules, as shown previously for small[13] [3] [14] [15] [16] and polymeric molecules, either unconjugated[17] or -conjugated[18]. From these, the study by Yao et al.[13] is particularly relevant for the present work, since it deals with the tuning of J-aggregation of a pseudoisocyanine dye at mica/water interfaces due to addition of 5% of an organic solvent (either 1-propanol or DI) in aqueous solutions. AFM and fluorescence microscopy showed that the morphology and fluorescence of films deposited onto mica, indeed correlate with the spectroscopic data.

Besides the morphology and fluorescence of films deposited onto mica, the surface free energy (SFE) has proven to correlate with solid-state properties of spin-coated films, and devices including them. For example, the SFE impacts the morphology, miscibility and segregation between adjacent layers, or layers and electrodes in organic solar cells (OSCs). [19] [20] [21] For example, a difference of around 10 mN/m in the SFE between layers (29.1 and 41.1 mN/m) promotes a poor miscibility, producing a slightly larger phase-separated film morphology. [20,22,23] However, when this difference decreases to around 2.5 mN/m (29.1 and 31.6 mN/m) penetration and diffusion of [6,6]-Phenyl-C_{71}-butyric acid methyl ester ($PC_{70}BM$) into the polymer region is promoted. [19]′[20,22,23] SFE also relates to the adhesive properties of the constituent layers of an OSC, impacting the mechanical stability of the device,[24] and it is also known to impact on the short circuit current and fill factor of these devices.[25] SFE has been used specifically to co-optimize the adhesion and power conversion efficiency by performing surface treatments of the buffer layer.[26]

For semiconducting polymeric films, the SFE (together with energy level and electrical conductivity) can be modified (i) by means of molecular structure, e.g. by changing the polymer backbone and lengths of alkyl side chains;[27] (ii) by doping processes, e.g. increasing the SFE of poly(3-hexylthiophene) (P3HT) films by doping;[28] and, in an easier way, (iii) by doing a Judicious selection of the polarity of the solvent mixture, which allows modulation of self-assembled aggregates (e.g. vesicles, rods etc.), as well as the optical properties of conjugated polymers and CPEs, as reviewed by Houston et al.[19] Variations in solvent polarity modify the relation between polarity and rigidity of both backbone and side chains of CPEs in solution, inducing conformational changes.[29]

Also, co-solvents allow gaining information on H-bonding interactions. For example, methanol−dimethylformamide (DMF) mixtures interfer with polymer-polymer and polymer-solvent H-bonding interactions, generating a nanoribbon morphology of poly(ethylene oxide) (PEO).[30] This occurs because mixed solvents generate preferential solvation of certain parts of the polymer, such as backbone and attached functional group, in certain component of the binary mixture.[31] Also, as reviewed by McDowell et al.,[32] co-solvents (also known as “additives” in the field of OSCs) provide an extra level of control over the two main parameters that control the OSC formation during solution processing: (i) thermodynamic parameters in solution, such as the solubility of donor and acceptor materials in the solvent(s), ease of crystallization/aggregation, and the mutual interactions between the solvents and the donor and acceptor solutes, and (ii) drying kinetics parameters, such as the vapor pressure of the solvents, and the deposition conditions that collectively define the drying kinetics of the mixture.[32] In our previous contribution[33] we used this approach, when analyzing the effect of imidazolium methylation on the SFE (estimated by means of contact angle goniometry) of imidazolium CPTs spin-coated onto plasma-activated glass, using water or a 50:50 v/v 1,4-dioxane-water (W-DI) mixture as processing solvents. It was observed that imidazolium methylation decreases the total SFE ($\gamma\boldsymbol{S}$) in ≈1mN/m, probably due to a more ordered structure, as suggested by previous studies on pentacene films which showed, by means of contact angle goniometry, that decreased film order increases $\gamma\boldsymbol{S}$ in less than 1 mN/m.[34] It is important to highlight that this result of SFE correlated with results fro X-ray diffraction (GIXD), synchrotron X-ray diffraction (XRD) and FTIR). In our previous work it was also observed that DI decreases $\gamma\boldsymbol{S}$ in 0.2-0.4 mN/m, increasing the polar

contribution (γS^{p}) and decreasing the dispersive contribution (γS^{d}) in 1-2 mN/m.[33] This information was discussed in terms of solvation and polymeric conformation within the films. Despite the cited contributions, and others using using Kelvin probe force microscopy (KPFM) or ultraviolet photoelectron spectroscopy (UPS) (e.g. [35] and its references), there are not yet available clear guidelines with respect to the structure of CPTs for designing high performance polythiophene-based interfacial layer materials.[19]

This work presents a study on the enhancement of J-like aggregation in solution- and solid-state, of a CPT due to the presence of 1,4-dioxane as cosolvent, in solution and solid-state.

The CPT, labelled PT1, is functionalized with isothiouronium units, which provide charge-assisted H-bonding (CAHB) capabilities, and a high sensitivity to the polarity and H-bonding capacity of the solvent. Water or a 1,4-dioxane-water 50:50 v/v mixture (W-DI) were used either as media or as processing solvent for deposition, because of their clearly different polarity/H-bonding capacity.

In solution, J-like aggregation enhancement of PT1 was revealed by fluorescence excitation spectroscopy, while in the solid-state, PT1 was deposited onto three anionic substrates: (i) drop-casted films onto glass were observed by means of fluorescence spectroscopy; (ii) spin-coated films onto plasma-activated glass were used to estimate the SFE by means of contact angle goniometry; and (iii) drop-casted films onto mica were used to observe the morphology by means of AFM.

To the best of our knowledge: (a) the use of the fluorescence excitation spectra to gain insight on J-like aggregation has been only reported by Deng et al.[10] and our previous work,[11] for water-soluble, conjugated fluorophore polymers, (besides studies on small molecules[12]); (b) there are not reports on the correlation between solution and solid-state J-like aggregation enhancement of a CPT due to the polarity/H-bonding capacity of the media/processing solvent, and (c) there are not reports on the effect of J-like aggregation on the SFE of films made of CPEs.

MATERIALS AND METHODS

Unless otherwise stated, all solvents and probe liquids used are of analytical reagent grade, commercially available and used as supplied (Sigma Aldrich). Deionized water was used for preparing the stock solutions.

Scheme 1a shows the skeletal structure of the cationic poly-3-(N-N-diethyl-S-iso-thiouronium)ethyloxy-4-methyl thiophene (PT1), as reported before.[36,37] As detailed before,[36] PT1 is assumed to have a DP ≈ 20-30 repeating units, after estimations made in this group,[38] [39] which are in agreement with those of cationic[40] and anionic[41] polythiophenes synthesized by different groups. PT1 is assumed to have a Đ ≈ 1–3, since this value was estimated consistently for CPTs in this[38] and other[41] [42] groups. About tacticity, PT1 is assumed to have mainly head-to-tail (HT) couplings between adjacent thiophene rings, through 2,5-linkages, because 3-alkoxy-4-methylthiophenes polymerized by a FeCl3 catalyzed reaction results in the formation of regioregular polymers with mainly HT 2,5-linkages.[43] [44] [45]

Schemes 1b-c show the expected H-bonding interactions between PT1 with glass or mica, respectively. Scheme 1d shows a model of a charge-assisted H-bond (CAHB) reported in molecules with structural similarity to PT1.

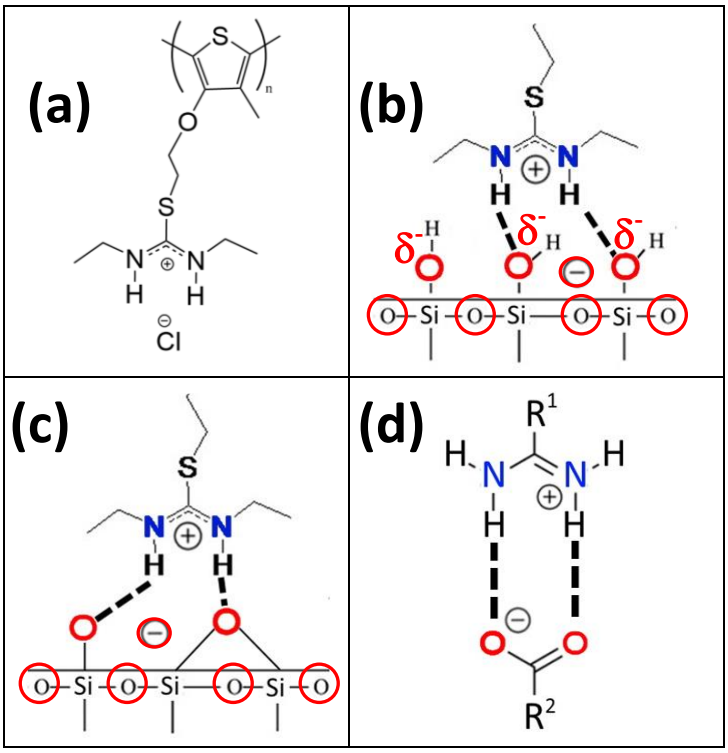

Scheme 1. (a) Poly-3-(N-N-diethyl-S-iso-thiouronium)ethyloxy-4-methyl thiophene (PT1), together with schemes of the H-bonding interactions (depicted as dashed lines) between PT1 and (b) plasma-activated glass and (c) freshly cleaved mica, modified from Matisons;[46] (d) shows an scheme of the $R_2^2(8)$ H-bonding geometry, often observed in CAHB frameworks, modified from [47]. Notice that in (b) the glass substrate is presented partially activated, having a partial surface concentration of Si–OH, and also Si–O–Si groups, interacting with the isothiouronium group in PT1 through CAHB, modified from Matisons,[46] Wu et al.[48] and Pooryousefy et al.[49]

Isothiouronium functionality

The seminal works on isothioureas stablished that these functional groups are able to act as H-bonding receptors in solvents that are prone to compete for intermolecular H-bonding, such as water and hydroxylic solvents, also known as "highly competitive" solvents.[50,51] The explanation reported is that by modyfing thiuoreas by S-alkylation generates a relatively large dipole moment and enhanced acidity of the NH residues present in thiourea, reason why isothiourea groups are improved binders to oxoanions, in comparison with thioureas.[50,52]

As shown in Scheme 1d, the Y-shaped structure of the isothiouronium functionality generates two-point H-bond donor capabilities when interacting with Y-shaped anions, such as the carboxylate group, or allows chelating of spherical anions (e.g. halides) and phosphates.[53]

Cationic isothioronium polythiophenes are also expected to show strong H-bonding donor capabilities at neutral pH, together with the optoelectronic properties from their conjugated nature. This is since the amino group in the thiourea functionality protonates in water at pH = 7, becoming positively charged which allows electrostatic interactions with anions and increasing solubility in water.[50,54]

Due to its cationic state, isothioureas also possess Lewis acidity, which allows their use as anion-binding units, [45] and are expected to avoid protonation or deprotonation in a good range of pH values, because of the pKa=21.1 of thioureas (in DMSO), however deprotonation may occur in the presence of a highly basic anion, normally F^-, causing dramatic spectral changes.[50]

As shown in Schemes 1b-c, this is valid also in the solid state, with the constituent cationic nitrogens possessing a surrounding electron density which participate in hydrogen bonds with certain substrates (e.g. ITO).[55] Therefore, these types of polythiophenes are ideal to study the solid-state organization onto substrates prone to establish H-bondings.

The Y-shaped isothiouronium functionality and the –OH and O present in plasma-glass or mica, possess what is known as the $R_2^2(8)$ H-bonding geometry. This pattern contains a total of eight atoms, two of them donors and two acceptors,[47,56] as shown in Scheme 1d.

As shown in Scheme 1d, the H-bonds stablished between the isothiouronium and oxygens, can be enhanced by the cationic charge of the isothiouronium group. This phenomenon is known as a *charge-assisted H-bond* (CAHB). CAHB is known to happen in ionic liquids (ILs), in which doubly ionic H-bonds occur when a H-bond forms between a cation. This occurs because in ILs the cations and anions are more complex than simple crystalline ammonium and halide species, which generates a richer and more diverse range of H-bonding.[57]

CAHB has been exploited to generate supramolecular materials constructed via intermolecular hydrogen bonds, in the pursue for more robust materials. For example, by pairing positively charged hydrogen bond donor groups, such as guanidinium, amidinium, or imidazolium, with a range of anions.[47] An example involving anionic oxygen H-bonding acceptors, are the H-bonds present between an aromatic nitrogen base and an organic or phosphorous acid. Other examples are provided in the review of Hunt et al. [57]

Solvent systems

DI is miscible with water in all proportions, it is a non–polar aprotic solvent with a boiling point and density similar to water, see Table 1. However, DI is interesting since its dielectric constant is significantly lower than that of water. As a consequence, water and W-DI have reported values of 80.38 and 36.89.[58] DI also is capable of accepting two hydrogen bonds, without donating any, and has a relatively bulky structure consisting of ether groups can disrupt the normal structure of water, which causes a disruption of the H-bonding donor-acceptor ratio.[59] Also, water and DI are considered to have strong and moderate H-bonding capacities, respectively, according to the Hildebrand scale.[60]

Density functional theory studies showed that complexation of molecules can be modulated by changing the presence of DI in water.[59] Also, Burrows et al.[61] reported molecular dynamics (MD) simulations of the interactions between tetramers of an anionic phenylene-fluorene copolymer, in water or a 1,4-dioxane-water 50:50 v/v mixture, which showed that DI breaks up aggregates due to a "coating" effect that displaces water from the immediate environment of tetramers. Such displacement would then limit the accessibility of water to the oligomers, while the sulfonate groups would be preferably solvated by water. The authors hypothesized that the DI coating effect: (i) would reduce the interaction between oligomers (in comparison with the interactions present in water), breaking up the polymer aggregates, and (ii) would prevent the interactions between the (anionic) sulfur side chains of the oligomers.

Such coating effect is in agreement with the experimental study by Luong et al.,[62] who analyzed the evolution of water H-bonded, collective network dynamics, in water-DI mixtures, with mole fractions of water ranging from 0.005 to 0.54. It was observed that heteromolecular water-DI H-bonding dominates only in the water diluted region, while the progressive addition of water, beyond a mole fraction of water of 0.1, generates a bulk-like, intermolecular, three-dimensional H-bonded water network dynamics.

Also, DI has been also used as cosolvent in research involving OSCs.[63,64]

In the present work, the use of W-DI causes co-solvation to play a central role on the solution interactions under study. Co-solvency is a complex phenomenon that involves several factors in the interactions between solvents (or co-solvents) and solutes, requiring knowing experimentally solvation parameters of the molecules under study.[65] [66] [67] Due to the lack of experimental data for CPEs in general, this compromises the possibility of performing quantitative solvation studies on CPEs. This is clearly explained and exemplified in the article by Burrows et al. [61]

Table 1 shows some relevant physical-chemical properties of water and the 50:50 v/v mixture of water and 1,4-dioxane (W−DI).

Table 1. Values of some physical-chemical parameters of the solvents used (at 20° or 29° C). The table also shows the H-bonding capacities of each pure solvent, according to the Hildebrand scale, together with the values of the H-bonding interactive force (δH) of the Hansen solubility parameters of each pure solvent.

Solvent	*Density (g/cm^3)*	*Boiling point (° C)*	*Dynamic Viscosity (mPa s)*	*Dielectric constant*	*Relative Polarity* †	*Refractive index*
Water	0.99[68]	100[69]	*0.754[70]	80.38[71]	1	*1.33[70]
W-DI	1.03[72]	87.83[69]	*1.4[70]	36.89[71]	0.46	*1.40[70]

* At 29 °C

† Ratio "Dielectric constant of cosolvent mixture/Dielectric constant of water"

Table 1-cont.

Solvent	*Hydrogen bonding donor capacity **	*δD Dispersion †*	*δP Polar †*	*δH Hydrogen bonding †*
Water	Strong	15.5	16.0	42.3
DI	Moderate	17.5	1.8	9.0

* [73]

† [74]

PT1 solutions and steady-state spectroscopy

The experimental procedures were performed as reported before in regard to PT1 solutions[11,33] and UV-Vis/fluorescence spectroscopy measurements,[11] please see the Supplementary Information of the present work for details. All spectroscopic data was analyzed and plotted with aid of the SpectraGryph optical spectroscopy freeware (Version 1.0.3).[75]

Drop-casted films on glass and fluorescence microscopy

In regard to the drop-casted films on glass, the films were obtained by drop-casting 3 μL of 0.2 mg/mL solutions of PT1, either in water or W-DI, on MatTek glass bottom dishes.

This concentration was selected after studies with imidazolium CPTs from this[39] and other[76] groups. The solutions were filtered through a 5-6 μm PTFE membrane, to minimize the possible presence of dust particles. The drops were allowed to dry at ambient temperature in a sealed container overnight.

Fluorescent microscopy was performed on a widefield Nikon Eclipse Ti2-E with a Hamamatsu sCMOS Orca Flash4.0. A 20x Nikon CFI Plan Apo Lambda NA 0.75 objective was used to capture images. Fluorescence excitation was performed using the Lumencor Spectra X LED system at 395nm while fluorescence emission was recorded using optical filters 515/30nm and 632/60nm. All acquisition parameters were kept consistent across samples. Micrographs from different samples or locations within a sample were taken from the center of the glass-dish.

Image analyses were performed with the freeware ImageJ-FIJI.[77] All the images analyzed had the same dimensions (≈665x663 μm), with slight variations required in order to avoid saturated pixels via the cut-off point value selected (details ahead).

Flat field correction was performed on all images to correct for uneven illumination.[78] After flat-field correction, the light intensity (in greyscale values) of the 16bit images was measured within a threshold 0-50,000. The maximum of 50,000 was set as the cut-off point in order to avoid measuring saturated pixels. The micrographs obtained are 16bit TIFF, meaning the maximum signal from a pixel is 65,536.

The analyses were performed using the maximum signal as a point of analysis, despite the presence of few super-bright aggregates, which do not give an overall representation of the whole field of view. Saturated aggregates were avoided because they disrupt the mean, maximum, minimum and median of the intensity from each micrograph. The maximum relative standard deviation (RSD) of the grey value within the micrographs was 26%.

The comparison between processing solvents (water or 1,4-dioxane mixtures) was done via the mean grey value of the micrographs (the exact same conclusions are obtained if the maximum, minimum or median values are used to compare).

Spin-coated films on glass, contact angle goniometry and surface free energy estimations

The preparation of blanks and polymeric samples, and posterior contact angle (CA) meaurements and estimation of surface free energy (SFE) from blanks and PT1-films, were performed as reported before.[33] Details can be found in the Supplementary Information.

Drop-casted films on mica and atomic force microscopy (AFM)

In regard to the drop-casted films, freshly cleaved mica carries a slightly negative charge in presence of water, with a density of 0.57 ions/nm, reason why it is possible to adsorb phospholipids without any further

modification of the mica surface.[79] Therefore, mica was used as an anionic model surface to study the role of the polarity/H-bonding capacity of the solvent on the interactions between PT1 and an anionic counterpart during the drying process, studying qualitatively the self-assembly of molecules without the centrifugal force of spin-coating. This study was performed following the reasoning of previous works studying the interaction between mica and cationic unconjugated polyelectrolytes,[17] or conjugated polyelectrolytes (CPEs) of a cationic nature.[18,80]

The films were obtained by drop-casting 3 μL of 1 mM (0.24 mg/mL) solutions of PT1, either in water or W-DI, on freshly cleaved mica surfaces. This concentration was selected after the work by Kesters et al., using cationic polythiophenes.[76] The solutions were filtered through a 5-6 μm PTFE membrane, to minimize the possible presence of dust particles. The drops were allowed to dry at ambient temperature in a sealed container overnight. The AFM measurements were performed in a class 100 clean room, under ambient conditions, in tapping mode, using silicon cantilevers (≈225 nm length, ≈20 nm tip-height, resonance frequency≈84 kHz). The AFM micrographs were processed with aid of the freeware Gwyddion.[81]

RESULTS

Figure 1 shows the absorption, excitation and emission spectra of PT1 in water and W-DI at increasing concentrations ranging from 0.1 mM (0.024 mg/mL) to 1 mM (0.24 mg/mL). Besides gaining information about the ground (S0) and excited (S1) states with UV-Vis and fluorescent emission, respectively, fluorescent excitation spectra allows detecting the spectral response to pi-pi stacking of the aromatic groups present in water-soluble conjugated fluorophore polymers.[10]

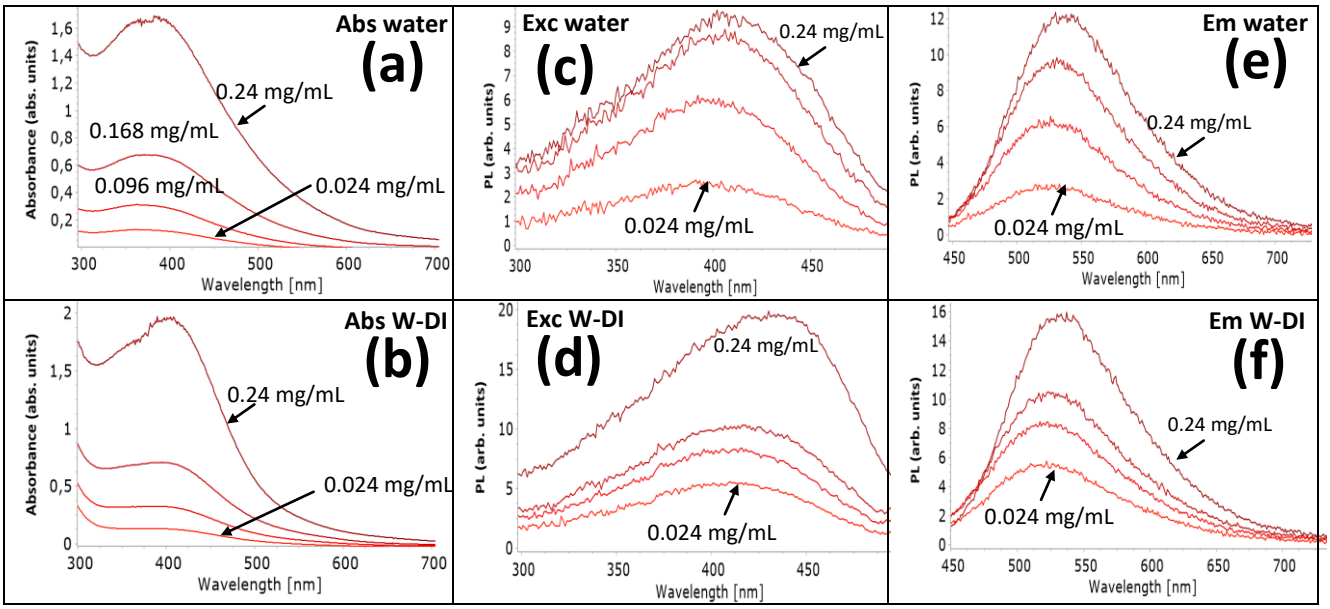

Figure 1. Absorption (a, b), excitation (c, d) and emission (e, f) spectra of PT1 in water and W-DI, respectively in each type of spectra, in the concentration range 0.024 to 0.24 mg/mL. Each figure shows the same concentrations.

The single absorption and fluorescence bands observed in Figure 1 suggest that the aggregation of PT1 is mainly related to changes in its conformation, rather than a loss of solubility, since studies on nucleation and growth of diluted poly(3-Hexylthiophene) (P3HT) have shown that single bands in absorption and fluorescence suggest well dissolved, disordered states. In comparison, emergence of more absorption and fluorescence bands have been associated with poor solubility and increases in the conjugation length of P3HT, and also pi-pi inter-chain stacking.[82]

The red shifts in fluorescence due to increased PT1 concentration observed in both solvents (Figures 1e,f), indicate different types of aggregation modes, associated with the tilt angle between adjacent pi-delocalized systems, as observed before in small and polymeric conjugated molecules.[1,5,6,10] In the case of the maximum in PL emission (λ_{em}), these shifts have been related to conformational changes in the

backbone of polythiophene copolymers,[18] and also to conformational changes, aggregation, and solvatochromic effects of semiconducting polymers.[83]

In Figures 1c,d is observed that as expected, in both solvents, the fluorescence intensity increase with increasing concentrations. Figures 1a,b show that the absorption of PT1 in both solvents has similar absorbance values, which is in agreement with the similar values of molar absorption coefficients of PT1 estimated in water (1,692 M/cm) and W-DI (1,871 M/cm).[36] In the case of fluorescence, Figures 1e,f show that W-DI generates much larger intensity values. This is in agreement with the quantum yield (Φf) values of PT1 in water (0.35) and W-DI (1.04).[36] Quantum yield values are informative about charge-transfer states and radiative and nonradiative processes as a function of solvents,[84] [31] [85] changes in Φf are associated with different π-conjugations and/or triplet formation of conjugated ring molecules such as thiophenes. Therefore, our results show that the presence of DI affects the pi-pi interactions between adjacent thiophene rings, probably because of improved solvation.

In the case of the Stokes shift (Δυ) values, these allow comparing relaxation energies, indicating the energy difference between the (λ_{max}) and fluorescent emission (λ_{em}).[86] Stokes shifts are informative about possible specific solvent−fluorophore interactions.[87] [88] [89] [11] Large Stokes shifts in oligo and polythiophenes, indicate effective nonradiative relaxation pathways along and between the chains.[85]

In this regard, as we reported before in diluted and concentrated solutions,[36] [11] PT1 has larger Stokes shifts in water than in W-DI. Therefore, our results indicate a clearly different conformations of PT1 in each solvent, with water possibly promoting effective nonradiative relaxation pathways along and between the chains (i.e. intra- and inter-chain relaxation).

Figures 1a,b and 1e,f show that neither the absorption nor the emission bands get distorted with increasing concentrations. However Figure 1d shows that in W-DI aggregation (large concentration) causes a distortion in the fluorescence excitation spectra, caused because of a slight decrease in intensity in the 350-400 nm range, together with an increase around 450 nm, which generates an excitation spectrum with a slight skewness to higher wavelenght values. Oppositely, Figure 1c shows that in water an increase in polymer concentration does not distort the Gaussian band shape of the excitation spectrum. This could be explained in terms of a possible coating effect of DI. As mentioned before in this work, the experimental work by Luong et al.[62] and the molecular dynamics (MD) study by Burrows et al.[61] could help in providing a qualitative explanation to the distortion in the excitation spectra due to PT1 concentration.

These works propose, respectively, (i) the existence of a collective network dynamics in water-DI mixtures, with bulk-like, intermolecular, three-dimensional H-bonded water network dynamics at high mole fractions of water, and (ii) a coating effect of DI (in 50:50 v/v water-DI mixtures), capable of displacing water from the immediate environment of anionic tetramers, limiting the accessibility of water to the oligomers, placing water instead near to the anionic groups and counter-ions. Such water displacement would prevent interactions between the anionic sulfur side chains, reducing the interactions between oligomers (in comparison to those present in water), breaking-up the pi-stacked aggregates.

As postulated in our previous contribution,[11] making an analogy to lignosulfonates,[10] at high PT1 concentrations, the presence of organic cosolvents seem to increase the number of J-like aggregates due to an increased number of isolated (non pi-stacked) aromatic groups, because of displacement of water from the immediate environment of the polymeric chains, promoting intra-chain energy transfer, with water solvating preferentially the isothiouroniums and counter-ions. This would promote intra-chain interactions, which dominate in J-like aggregates[6] (see scheme 2b). This could explain the observed shrink in the intensity of the excitation band at shorter wavelengths, whereas the bands at longer wavelengths are strengthen,[10] generating the distortion in the excitation spectrum observed in Figure 1d.

Oppositely, water would promote pi-pi stacking of thiophene rings, promoting inter-chain interactions (see scheme 2a). This would cause an equilibrium between “isolated” aromatic groups and polydisperse J-like aggregates, with the ratio of the “isolated” aromatic groups to the J–aggregates not changing with increasing concentrations. This could explain the lack of distortion in the excitation spectra with increasing concentrations. This invariance of the excitation spectra with increasing polymer concentrations suggest that the J-like aggregates have a low aggregation number.[10]

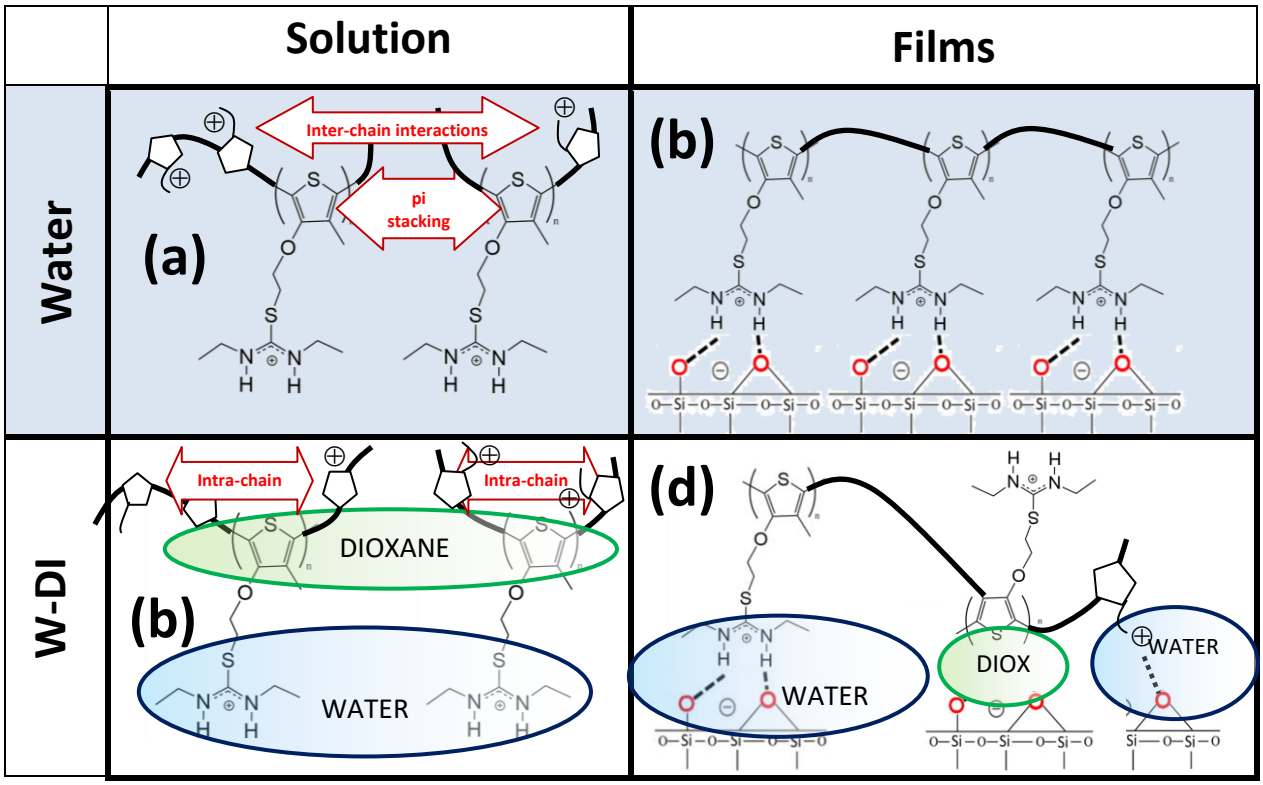

Scheme 2. Possible polymer-polymer interactions for concentrated solutions in (a) water or (b) W-DI; and possible polymer-substrate interactions for films processed from (c) water or (d) W-DI. Some thiophene rings are shown as simplified pentagons with an attached cationic charge.

In regard to our results in the solid-state, water and W-DI have different boiling points (100 and 87.8° C, see Table 1), which is expected to generate different drying kinetics.[32] Therefore, the differences observed in the drop-casted films on mica are related to the molecular interactions between PT1 and mica, and also because of a difference in the drying kinetics of the drop-casted films processed from water or W-DI.
These differences in boiling point are expected to relevant for the drop-casted films (i) on glass (used to visualize the fluorescence) and (ii) on mica (used to visualize the morphology). The possible effect of the boiling point of each solvent is discussed ahead. In the case of spin-coated films, due to the fast evaporation caused by the spinning element, the differences in boiling points can be considered negligible.

Fluorescence microscopy of drop-casted films onto glass

Figure 2 shows typical micrographs from drop-casted films of PT1 from water, and mixtures of 1,4-dioxane with water in proportions of 30:70 v/v and 50:50 v/v (i.e. W-DI). The numbers indicate the average of the maximum signal (grey values) of the images (see Table S2 for all the values). Figure S1 shows repetitions of micrographs from random samples/positions.

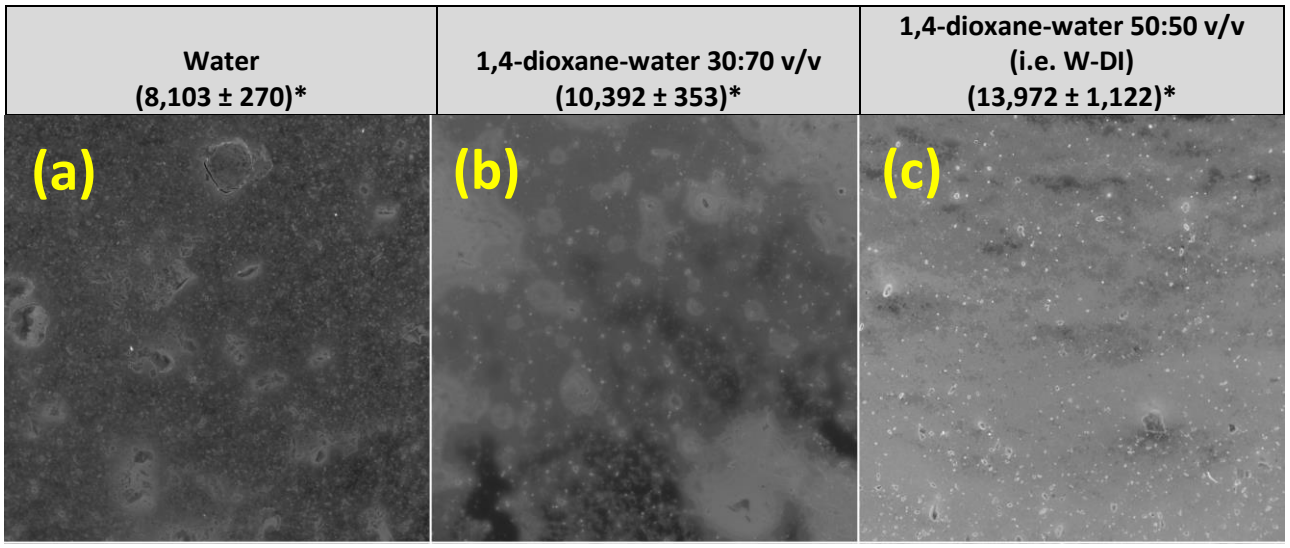

Figure 2. Fluorescence micrographs of the PT1 (0.24 mg/mL) drop-casted films on glass from (a) water; (b) 1,4-dioxane 80:20 v/v and (c) 1,4-dioxane-water 50:50 v/v mixture (i.e. W-DI).
*Numbers in each micrograph indicate the average value (grey values) of the maximum signals through the image.

Figure 2 shows that regardless the processing solvent, the morphology and fluorescence give evidence of the coverage of PT1. These micrographs are clearly different from those obtained from the glass blanks, which are completely black, showing any fluorescent emission (result not shown). Notice that despite not showing any fluorescence visually, the blanks generate an average maximum grey value of 988.7, which is much smaller than those values obtained from the PT1-films, ranging between 8,000 to 14,000 depending on the processing solvent (See Table S2).

Figure 2a shows that when water is used as processing solvent, it is obtained an amorphous morphology with islands of PT of different sizes, together with small aggregates (observed as bright dots) present through the whole surface. It is also observed a halo of light surrounding the bigger structures, and the presence of some super-bright small aggregates.

Figure 2b shows that when DI is present in 30% in the processing solvent, it is generated a similar structure to that obtained from water, with big and small structures. However, the halo of light surrounding the bigger structures is considerably larger. The small dots are also observed, with similar distribution and brightness to those observed in the films obtained from water. Same as in the films processed from water, some super-bright aggregates are observed. As shown at the top of the middle column, these films are in average approximately 28% brighter than those obtained from water.

Finally, Figure 2 shows that when DI is present in 50% (i.e. for films obtained from the W-DI mixture), the halos of light become present through the whole micrograph, with the small dots becoming noticeably brighter than those present in the other two types of films. The brightness of these structures is similar to the super-bright structures observed in the other two types of films. As shown at the top of the column, these surfaces are in average approximately 72% brighter than those obtained from water.

These results are in agreement with those of aggregation in solution, which showed a larger quantum yield in the W-DI solutions. Also, these results show that the presence of DI in enhancing the fluorescence of PT1 aggregates (perhaps due to an enhancement of J-like aggregation) remain in the solid-state.

The lower boiling point of W-DI (see Table 1) is expected to promote pi-pi stacking during drying, because its faster evaporation increase the % of water in the W-DI mixture. This in turn is expected to increase pi-pi stacking, and therefore inter-chain transfer. However, the largest brightness of the films processed from W-DI suggest improved intra-chain energy transfer. In order to observe morphological changes in the films due to the processing solvent, it was conducted an AFM study of films drop-casted onto mica, because of (i) the higher resolution of this microscopy and (ii) the larger cationic character of mica over the glass in the fluorescence microscopy dishes.

Morphology of drop-casted films onto mica

Figure 3 shows typical topography AFM micrographs of drop-casted PT1-films formed on mica from 0.24 mg/mL solutions in water or W-DI.

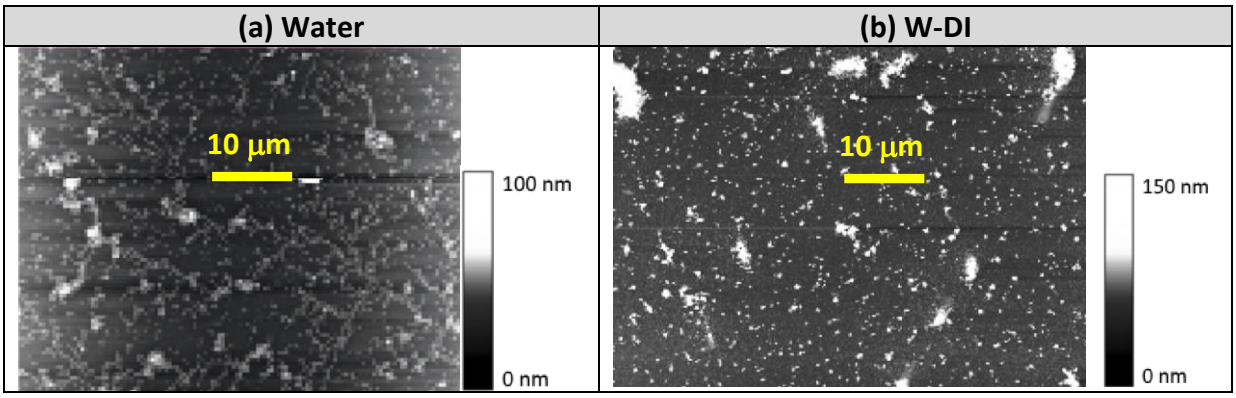

Figure 3. Topography-AFM micrographs of drop-casted films from PT1 solutions (0.24 mg/mL) in (a) water or (b) W-DI.

Figure 3a shows that when the film is drop-casted from water, the film obtained has a branched structure, with some origin points for branching, having an almost dendritic structure. On the other hand, the film drop-casted from W-DI presents a noticeably different morphology, with isolated islands of PT1, lacking any branched structure, with a larger average thickness.

Our results are in agreement with Gutacker et al.,[18] who reported a loss of dendritic structure when switching from water to methanol as processing solvent. The fractal dendritic structure obtained from water is similar to that reported for films of a cationic thiophene-fluorene copolymer on mica from aqueous solution.[18] Dendritic structures also resemble the typical morphology of crystalline polymer thin films formed through a diffusion-limited aggregation (DLA) mechanism.[90] DLA morphologies have been accurately simulated by computational means, for random metal-particle aggregates.[91,92] As described by Friedlander in simulations of stochastic aggregation of aerosols,[93] DLA is one of the three kinds of agglomerate formation, together with ballistic aggregation (BA) and reaction-limited aggregation (RLA). The DLA model produces clusters exhibiting complex scaling properties, while in the BA the free particles move ballistically at randomly chosen directions and obey the same sticking rules as the DLA model.[94]

In the case of the PT1-films processed from water, the branched structure observed in Figure 3a resembles more BA rather than DLA.

In regard to effect of DI, the change from dendritic into islands morphologies due to DI is similar to the works by Tumbek and Winkler,[95] [96] in which a change from DLA into a morphology consisting of isolated islands was described for the growth of hexaphenyl (6P), a rod-like organic molecule, due to decrease in the surface roughness of the substrate (mica). Such islands-like morphology was labelled as attachment limited aggregation (ALA).

Therefore, in the present work DI causes a switching from DLA or BA, into ALA. However, regardless the possible specific aggregation mechanism, there is a clear difference in the structures PT1 forms when processed from water or W-DI. Furthermore, our results are in qualitative agreement with the studies of Yao et al.,[13] focused on the extent of J-aggregation and surface morphology changes due to the processing solvent (either water or its mixtures with DI or 1-propanol), when depositing a cationic (N-ethyl) pseudoisocyanine dye at the solvent/mica interface. It was observed that the presence either organic co-solvent caused a proportional decrease in the size and coverage of the J-aggregate islands. The authors hypothesized that a combination of pi-pi stacking and electrostatic interactions were primarily responsible for the characteristic organization of dyes at the mica interfaces, with two main possible arrangements: (i) dye molecular planes parallel to the mica surface or (ii) molecular plane perpendicular to the surface, with the latter being more favorable and likely to happen, due to epitaxial match. It was proposed that organic solvents would increase the solubilization of the dye, reducing the driving force for adsorption, decreasing the amount of the interfacial dye molecules in both lateral and vertical dimensions.[13] It is important to notice that because of the AFM used in this reference is in the mica/solvent interface, there is a competition between the solvent and mica for the dyes. This competition is also present, in a smaller extent, in the drop-cast produced in the present work, since it is reasonable to assume that during the

drying of the film, the solvent still plays a role in the conformation of PT1, and therefore guides partially the solid-state morphology.

The morphologies of PT1-films from both processing solvents are also in agreement with adsorption isotherms for poly(AM-MAPTAC) polyelectrolytes on mica, in which was observed that for larger number of cationic groups in the polyelectrolyte (i.e. larger cationicity), the polyelectrolyte adopted a flatter configuration on the surface.[17]

Despite the obvious differences between dyes and polymers, our results suggest that when using water as processing solvent, the media is optimal for allowing H-bonding between the isothiouronium and the anionic groups in mica (see scheme 2c). As mentioned in the materials section, due to S-alkylation, isothioureas ara capable to form H-bonding in highly competitive media such as water.[50,51]

Therefore, the polymeric chain is capable of, for example, moving ballistically at random directions (i.e. via the BA and/or DLA mechanisms), generating the dendrimeric structures observed in Figure 3a.

On the other hand, the presence of DI decreases the driving force for adsorption in some isothiouronium units, due to the coating effect of DI (See scheme 2d). DI would then decrease the number of isothiouronium-mica cation-anion contacts. This would cause a preferential growth in J-like islands, probably similar to those described by the ALA mechanism, vanishing the dendritic structure observed in the films drop-casted from water.

Notice that the lower boiling point of W-DI (see Table 1) is expected to promote an overall faster drying process, which could also impact on the lack of movement of PT1 (switching from ballistically into attachment-limited), the extent of each effect (coating of DI and drying kinetics) is beyond the scope of the present work and under study in our research group.

Contact angle goniometry and SFE of spin-coated films onto plasma-activated glass

Table 2 shows the average contact angle (CA) values of the probe liquids on the three blank-surfaces (see supplementary information for details on these surfaces): (i) plasma-activated glass (plasma-glass), (ii) plasma glass spin-coated with water (glass-water) and (iii) plasma glass spin-coated with DI (glass-DI). Table 3 shows the SFE estimations (with OWRK and Wu models) of the three blanks and the 1- and 5-deposited PT1-films. The values of the polar ($\gamma S\boldsymbol{p}$) and dispersive ($\gamma S\boldsymbol{d}$) contributions are also shown.

Table 2. CA values between the four probe liquids on (i) plasma-activated glass (plasma-glass), (ii) plasma-glass spin-coated with water (glass-water) and (iii) plasma-glass spin-coated with DI (glass-DI).

Blank surface / Probe liquid	Plasma-glass CA (°) ± SD*	Glass-water CA (°) ± SD*	Glass-DI CA (°) ± SD*
Glycerol	37.55±7.35	39.39±6.6	44.44±5.39
Ethylene glycol	21.87±5.14	24±5.82	30.05±2.76
Formamide	7.23±1.94	14.4±1.57	16.76±1.87
Diiodomethane	38.46±3.86	43.22±3.71	43.35±2.66

*SD values based on at least triplicates (see ESI)

Table 3. Total SFE ($\gamma\boldsymbol{S}$) and its polar ($\gamma S\boldsymbol{p}$) and dispersive ($\gamma S\boldsymbol{d}$) components according to OWRK (with data from glycerol and diiodomethane) and Wu's (with data from the four probe liquids) models.

	SFE / Surface	OWRK $\gamma\boldsymbol{S}$ (mN/m)	OWRK $\gamma S\boldsymbol{p}$ (mN/m)	OWRK $\gamma S\boldsymbol{d}$ (mN/m)	Wu $\gamma\boldsymbol{S}$ (mN/m)	Wu $\gamma S\boldsymbol{p}$ (mN/m)	Wu $\gamma S\boldsymbol{d}$ (mN/m)
Blanks	Plasma-glass	54.13	13.76	40.38	54.89	13.64	41.25
	Glass-water	52.39	14.43	37.95	53.16	14.1	39.06
	Glass-DI	49.86	11.98	37.89	51.78	12.44	39.34
PT1	1-deposition from water	55,47	11,16	44,31	55,52	11,05	44,47
	1-deposition from W-DI	52,87	10,6	42,28	54,42	11,3	43,12
	5-depositions from water	50,37	6,1	44,27	54,35	9,01	45,33
	5-depositions from W-DI	50,32	7,45	42,87	53,42	9,31	44,11

The data presented in Table 3 (shown visually in Figure S2) shows that both models (OWRK and Wu) do not generate the same SFE values, and also that the OWRK model generates larger differences between the 1- and 5-deposition films. However, concerning the effect of solvent and number of depositions, the OWRK model generates the same trends than Wu's model.

Therefore, for the sake of simplicity, and also to allow comparing with previous reports (all the references cited ahead used Wu's model), Figure 4 shows only the SFE values estimated with Wu's model for blank surfaces and polymeric films.

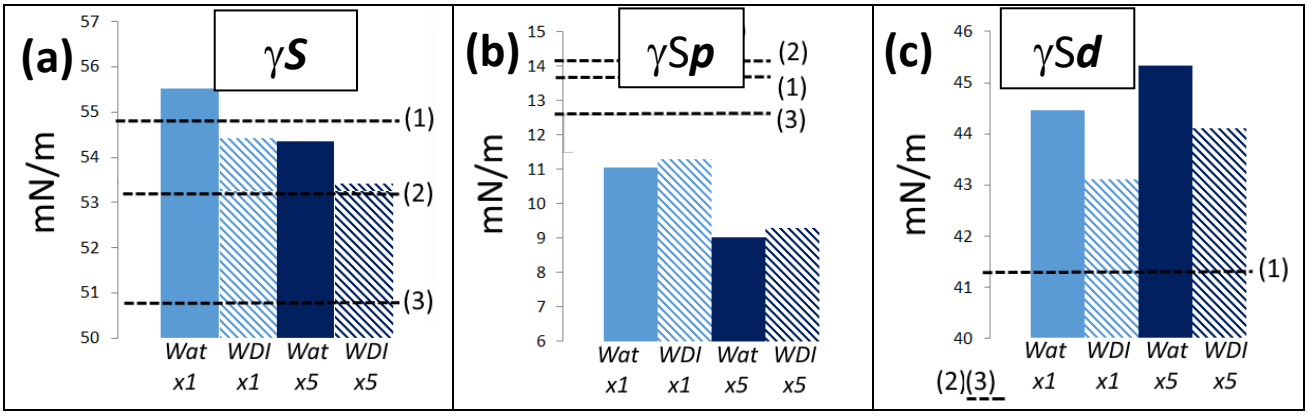

Figure 4. Estimated values of (a) the total SFE (γS) and its (b) polar (γS^p) and (c) dispersive (γS^d) contributions, as estimated using the Wu model, from films with 1-deposition (light blue) or 5-depositions (dark blue) of 0.24 mg/mL PT1 solutions, processed from water (solid color bars) or W-DI (dash-patterned bars). Dashed horizontal lines indicate the γS, γS^p and γS^d values of the blank surfaces: (1) plasma glass, (2) glass-water and (3) glass-DI.

CA values of blanks

As show in Table 2, the average CA of formamide on the glass-water blank is 14.4°, which is 40% smaller than that reported previously from a glass substrate previously exposed to water (≈25°).[97] However, Table 2 also shows that the average CA from diiodomethane on the glass-water blank is 43°, which is similar to the CA of ≈45° reported for diiodomethane in the same reference.

On the other hand, in regard to the SFE estimations of the blanks, Table 3 shows that the OWRK and Wu models estimate a total γS ≈53 mN/m for the glass-water blank. This value is 15% smaller than that estimated for non-heated glass with controlled porosity (≈ 70 mN/m).[98] The difference between our CA values and those reported in the cited reference may be caused by a difference in the type of glass (e.g. borosilicate or soda lime glass, which have different smoothness, see [99]); and/or the difference in the drying conditions of each glass after being exposed to water. These factors (alone or combined) generate a different extent of hydration in each glass. The fact that diiodomethane generates a similar CA values in the present work and the work of Rymuszka et al.,[97] provide further evidence of this, since this probe liquid is expected to have a reduced sensitivity to hydration. Also, our estimations of SFE of glass-water are similar to those reported by Jakzuk et al.[98] Thus, it is reasonable to say that the glass-water blanks lie within the range of previously reported values of CA and SFE. Regardless, the experimental design of the present work allows in itself using the blanks to compare the effect of number of depositions or processing solvent.

Surface free energy of blanks and PT1-films

Figure 4a and Table 3 show that regardless the number of depositions, the PT1-films processed from water have a larger value of γS (by at least 1 mN/m) than the glass-water blank, while the films processed from W-DI show smaller differences with this blank, to the point of the 5-deposition films have a marginal difference with the blank.

In regard to the components of γS, Figure 4b shows that the γS^p of any blank is larger than those of the PT1-films. This suggests that the surface-concentration and/or -energy of the cationic (isothiouronium) units in the films is smaller than the –OH groups present in any of the blanks. Figure 4b also shows that the difference of γS^p between the PT1-films and the blanks is smaller for 1-deposition films, suggesting that more than one deposition causes a decrease in the surface concentration of the cationic isothiouronium units.

On the other hand, Figure 4c shows that regardless the number of depositions, the $\gamma S\boldsymbol{d}$ component of the PT1-films is always larger than any of the blanks, with water increasing this difference. This gives evidence of the presence of the hydrophobic components in PT1: thiophene rings and alkoxy spacer.

This is, the $\gamma S\boldsymbol{p}$ and $\gamma S\boldsymbol{p}$ contributions of the PT1-films are clearly different to those of the blanks, which gives evidence of the presence of PT1, besides providing some structural information (further analyzed ahead).

In regard to films of neutral- or conjugated-polymers previously reported, the 1-deposition films show $\gamma\boldsymbol{S}$ values of 55.5 and 54.4 mN/m when deposited from water and W-DI, respectively, which are values similar to those reported for doped-P3HT films on glass (54 mN/m) and $FeCl_3$-doped polypyrrole (PPy) films (55.4 mN/m).[28] These similarities have a qualitative nature, because the values reported in the references cited were obtained using different methods and substrates. However, this approach was indeed used in the review by Higgins and Wallace,[28].

Effect of number of depositions on the surface free energy

Figure 4a shows that regardless the processing solvent, a larger number of depositions decreases $\gamma\boldsymbol{S}$ in ≈1 mN/m. In regard to the magnitude and meaning of this difference, previous studies on pentacene films showed, by means of contact angle goniometry, that a decrease in film ordering causes an increase in $\gamma\boldsymbol{S}$ of ≈1 mN/m[34] (notice that this result was in agreement with (this result correlated with X-ray diffraction (GIXD), synchrotron X-ray diffraction (XRD) and FTIR).Therefore, our results could indicate that a larger number of depositions of PT1 increase film order. This hypothesis is reasonable due to the propensity polythiophenes (e.g. P3HT) have to form semi-crystalline domains in the solid state.

Figure 4b shows that the $\gamma S\boldsymbol{p}$ contribution is the one generating the difference in $\gamma\boldsymbol{S}$ due to a larger number of depositions, because oppositely from $\gamma S\boldsymbol{p}$, the dispersive contribution $\gamma S\boldsymbol{d}$ increases with the number of depositions. This suggests that improved ordering of the films decrease the contribution of the isothiouronium functionality to the polarity of the film.

In resume, from both processing solvents, depositing more than once decreases $\gamma S\boldsymbol{p}$ in ≈2 mN/m and increases $\gamma S\boldsymbol{d}$ in ≈1mN/m. Increasing depositions impacts mainly and negatively on the polar component of the SFE, while de dispersive component presents smaller changes, but of a positive nature. These trends suggest that more layers cause a decrease in the surface concentration of polar (cationic isothiouronium) species, while increasing, more slowly, the surface concentration of hydrophobic species (thiophene backbone and alkoxy spacer).

To gain further structural information it is useful to use the $\gamma S\boldsymbol{d}/\gamma S\boldsymbol{p}$ ratio. 1-deposition PT1-films generate $\gamma S\boldsymbol{d}/\gamma S\boldsymbol{p}$ ratios of 4 and 3.8, when processed from water or W-DI, respectively. These values are similar to those estimated in our previous contribution for films of imidazolium polythiophenes, ranging in values of 3-3.9.[33] However, our values are at least 90% larger than those reported from doped-films of P3HT deposited onto glass ($\gamma S\boldsymbol{d}/\gamma S\boldsymbol{p}$=1.42) or from doped-films of PPy deposited onto polyethylene terephthalate ($\gamma S\boldsymbol{d}/\gamma S\boldsymbol{p}$=2).[28,100]

5-deposition PT1-films generate even larger values of $\gamma S\boldsymbol{d}/\gamma S\boldsymbol{p}$, with values of 5 when processed from water and 4.7 when processed W-DI. This indicates that multi-deposited films reduce the impact of the isothiouronium cationic group (as discussed before).

These results indicate that despite 1-deposition PT1-films have values of $\gamma\boldsymbol{S}$ that are similar to previously reported doped-P3HT or -PPy films, such similarity does not hold in regard to the proportion of each of the components to the total $\gamma\boldsymbol{S}$, because the PT1-films generate larger values of the ratio $\gamma S\boldsymbol{d}/\gamma S\boldsymbol{p}$. Instead, the values of the $\gamma S\boldsymbol{d}/\gamma S\boldsymbol{p}$ ratio generated by 1-deposition PT1-films are similar to those estimated from *de-doped* films of P3HT (4.14).[28,100]

As discussed in our previous work,[33] these results indicate that that the cationic isothiouronium functionality in PT1 has a smaller contribution to the polarity of the films, in comparison with the contribution of regular dopants, probably due to the restricted mobility of the cationic functionalities attached to a CPE. Such restriction would also explain the results of the 5-deposition films, which show a larger value of $\gamma S\boldsymbol{d}$.

Effect of processing solvent on the surface free energy

Figure 4a and Table 3 show that for 1- and 5-deposition films, the presence of DI in the processing solvent decreases $\gamma S \approx 1$ mN/m. Same as discussed before, studies on pentacene films showed that decreased film order increases γS in less than 1 mN/m[34] (this result correlated with X-ray diffraction (GIXD), synchrotron X-ray diffraction (XRD) and FTIR). Therefore, in this case, the decrease in γS due to DI could also suggest DI increases the ordering in the film. Indeed, both effects are additive, since the 5-deposition films, processed from W-DI, present the smallest value of γS (≈53 mN/m). Therefore, assuming that the decreases in γS observed due to multi-deposition or the presence of DI is related with increases the ordering in the film, then it is reasonable to propose that DI increases the structuring, via the coating effect of DI which would promote hydrophobic interactions.

The decrease of γS in 1-deposition PT1-films due to DI (≈ 1mN/m), is at least 60% larger than that observed in films of imidazolium polythiophenes, in which case DI reduced γS in a range of 0.2 to 0.4 mN/m. [33] This may be related with the strongest H-bonding capabilities of PT1 in comparison with the imidazolium CPTs, and is further discussed ahead with the values of the γSp and γSd components.

The decrease in the dispersive contribution γSd caused by DI in the 1-deposition PT1-films (≈1.3 mN/m) is similar to that observed in films of imidazolium polythiophenes (≈1.2-2 mN/m), however, interestingly, the increase in γSp due to DI in the 1-deposition PT1-films (≈0.2 mN/m) is *one sixth* or less, than that observed in films of imidazolium polythiophenes (≈1.2-2 mN/m).[33]

In regard to the difference between the present work and that using imidazolium polythiophenes, the differences between these films (in regard to the extent of increase in γSp due to DI) may be related with the different H-bonding capabilities of PT1 and the imidazolium polythiophenes. In the case of the latter, the effect of DI blocking imidazolium-glass cation-anion interactions is larger than that in PT1, therefore causing DI to increase γSp in a larger extent than that observed in PT1-films, because the isothiouronium functionality with a double CAHB capabilities attaches to the glass in presence of DI, in larger extent than the imidazolium polythiophenes do.

The contact angle data from the most non-polar probe liquid has proven to be useful when analyzing the causes behind the increase in γSp due to the presence of DI, using a film with switchable surface polarity (or dispersity), made of of PPy electropolymerized in presence of dodecylbenzenesulfonate (DBS), on top of Si coated with Au/Cr.[101] Such film was electrochemically reduced or oxidized while measuring in situ the CA values of the least polar probe liquid they tested (dichloromethane). The reduced form of the films caused larger dichloromethane CA, due to a larger concentration of ionic (sulphonate) groups from the DBS, while the oxidized form caused smaller dichloromethane CA values, caused by a larger surface concentration of the hydrophobic dodecyl chains present in DBS.

Table S2 shows that the CA values of diiodomethane on 1-deposition PT1-films processed from water is 29.77±3.3°, which is ≈5° smaller than that on films processed from W-DI (34.46±6.2°). This difference is slightly larger to that observed in films of imidazolium CPTs, for which DI caused a reduction in ≈3°.[33] In the case of 5-deposition PT1-films, the effect of W-DI is smaller: the CA values of diiodomethane on films processed from water (29.88±4.8°) is ≈3.3° smaller than that on films processed from W-DI (33.15±2.4°).

Therefore, for films with both number of depositions, the presence of DI in the processing solvent increases the polarity of the films. This may be related to a larger concentration of "non-neutralized" cationic isothiouronium groups (using the concept of neutralization used in the adsorption of cationic polyelectrolytes on mica).[17] DI would cause PT1 to have a smaller available number of cationic units (i.e. its cationicity) to interact with mica, generating a surface with more cationic units, which would explain the larger CA values with the most non-polar probe liquid, diiodomethane, as shown in Schemes 1b-c.

This assumed surface concentration of cationic units obtained from each processing solvent is in agreement with adsorption isotherms for poly(AM-MAPTAC) polyelectrolytes on mica.[17] In that study, it was observed that for larger number of cationic groups in the polyelectrolyte (i.e. larger cationicity), which would be available to interact with mica, the polyelectrolyte adopted a flatter configuration on the surface (because of a larger number of cation-anion contacts).

As mentioned before, there is a lack of understanding on the effect of co-solvents on the drying-kinetics of conjugated molecules, and there are not studies using DI.[32] However, for the SFE data, the mechanism

we sketched in the scheme in Figure 4 also gives a possible explanation, [59] [61,62] in the same way we explained the results in our previous work:[33] a possible mechanistic explanation to our results would be that DI would cause a damping of the coulombic and/or H-bonding interactions between the isothiouronium groups and plasma-glass, and such screening effect would then decrease the number of isothiouronium-glass cation-anion contacts, causing a larger number of unattached isothiouronium groups, which could then contribute to the polarity of the films, increasing $\gamma S\boldsymbol{p}$ (see Figure 4d).

The detailed mechanism behind the different effect DI has on PT1 during the processing (i.e. deposition of films) involves thermodynamics of solvation in solution and drying kinetics, and requires further studies. This is currently under study in our group, by comparing solution-aggregation and solid-state properties of films made of imidazoliums and isothiouroniums, with the latter having different side-chain lengths, analogously to our previous studies in solution.[11,36]

CONCLUSIONS

Our results in solution, using the fluorescence excitation spectra, correlate with the solid-state properties of the films in regard to a possible enhancement of J-like aggregation due to the presence of DI. In solution and solid-state, our results can be explained qualitatively (following previous experimental and computational studies) as the result of a coating effect of DI, which causes selective solvation of the hydrophobic and hydrophilic parts of PT1 and the solid substrates, guiding the conformation in solution and the solid-state properties.

In solution, PT1 presents unstructured spectra in both solvents, which gets red-shifted in presence of DI, suggesting the aggregation of PT1 is mainly related to changes in its conformation, rather than a loss of solubility. Increased PT1 concentration increases absorption in similar extent, due to similar values of molar absorption coefficient between solvents. In the case of PL emission, the presence of DI causes a larger increase of intensity due to increasing PT1 concentrations, due to a larger quantum yield, indicating that DI affects the pi-pi interactions between thiophene rings, probably because of improved solvation. W-DI generates smaller values of Stokes shift, suggesting clearly different PT1 conformations in each solvent, with water possibly promoting effective nonradiative relaxation pathways along and between the chains. The fluorescence-excitation spectral bands get distorted in W-DI due to concentration, generating an spectrum with skewness to higher wavelength values. Oppositely the spectra in water remain invariant at high concentrations. This seems to be related with selective solvation of DI, displacing water in between polymeric chains, increasing the number of isolated aromatic groups, promoting in turn an increase in the degree of J-like aggregation (i.e. increased intra-chain interactions) via reducing pi-pi stacking.

To the best of our knowledge, besides our previous contribution,[11] there is only one report about detecting J-like enhanced aggregation of polythiophenes in solution,[6] and two reports on using the excitation spectra to analyze H-J aggregation, for a polymer[10] and a dye.[12] However, any of these reports provided evidence correlating solution and solid states.

In this regard, in solid-state, DI seems to decreases the Coulombic and/or H-bonding interactions between the isothiouronium groups and the anionic substrates, decreasing in turn the number of isothiouronium-glass cation-anion contacts, causing a larger number of unattached isothiouronium groups, which could then cause changes in the solid-state morphology, increasing fluorescence, switching the type of aggregation mechanism and increasing the polarity of the films.

Firstly, the drop-casted films on glass processed from W-DI generate almost twice the fluorescence intensity than those films processed from water. Secondly, in the case of the drop-casted films onto mica, the films processed from water have a dendritic structure similar to diffusion-limited aggregation (DLA) or ballistic aggregation (BA), while the presence of DI in the processing solvent generates a morphology consisting of islands of PT1, similar to a morphology previously described as attachment limited aggregation (ALA), analogously to the tuning of J-aggregation of small conjugated molecules in solution and solid-state,[16] caused by the lower binding efficiency of these molecules onto mica because of the presence of organic solvents. Our results provide insight on the relationship between polymer and solvent with the type of aggregation occurring onto mica substrates. This has been scarcely reported previously in literature devoted to CPTs, e.g.[18].

Finally, in the case of spin-coated films on plasma-activated glass, the presence of DI in the processing solvent slightly increases $\gamma S\boldsymbol{p}$, and decreases $\gamma S\boldsymbol{d}$. The decrease DI causes in $\gamma\boldsymbol{S}$ ($\approx$ 1mN/m) is at least 60%

larger than that observed in previously reported films of imidazolium polythiophenes.[33] On the other hand, DI increases γS^{p} in a much smaller extent to that observed in imidazolium polythiophenes films,[33] which seems to be related with stronger CAHB capabilities in the isothiouroniums over imidazoliums. The contact angle (CA) values of diiodomethane suggest that DI decreases the number of cation-anion contacts between the imidazolium group and glass, causing therefore a larger number of unattached isothiouronium groups, which could then contribute to the polarity of the films.The presence of DI and the increase in number of depositions are additive, since the 5-deposition films processed from W-DI present the smallest value of γS^{s} (≈53 mN/m). This suggest a possible increase in the ordering of the film by either treatment, which is reasonable given the properties of hydrophobic polythiophenes such as P3HT to form semi crystalline arrangements.

The tuning of solid-state properties of polythiophenes has been scarcely reported in literature,[19] same as the study of co-solvents as morphology-directing agents for solution-processed organic optoelectronic devices.[32] Our results provide knowledge on controlling the aggregates of CPTs in the solid-state, which could be useful for predicting and designing specific mesoscopic architectures.

AKNOWLEDGEMENTS

Sergio E. Dominguez deeply acknowledges: (i) The Magnus Ehrnrooth Foundation for the Postdoctoral Grant 2020; (ii) the Mexican National Council for Science and Technology (CONACyT) for the scholarship no. 310828, (iii) the Turku University Foundation (Turun Yliopistosaätiö), (iv) the Real estate Foundation (Kiinteistösaätiö), (v) the partial support from the Finnish National Doctoral Programme in Nanoscience (NGS-NANO) and Doctoral Programme in Physical and Chemical Sciences (PCS) from University of Turku, (vi) the Cell Imaging and Cytometry Core, (Turku Bioscience Centre, University of Turku and Åbo Akademi University and Biocenter, Finland), for the fluorescence microscopy observations, and (vii) the help of Lauri Marttila with the Gwyddion software.

REFERENCES

[1] M. Son, K.H. Park, C. Shao, F. Würthner, D. Kim, Spectroscopic Demonstration of Exciton Dynamics and Excimer Formation in a Sterically Controlled Perylene Bisimide Dimer Aggregate, J. Phys. Chem. Lett. 5 (2014) 3601–3607. https://doi.org/10.1021/jz501953a.

[2] M. Más-Montoya, R.A.J. Janssen, The Effect of H- and J-Aggregation on the Photophysical and Photovoltaic Properties of Small Thiophene–Pyridine–DPP Molecules for Bulk-Heterojunction Solar Cells, Advanced Functional Materials. 27 (2017) 1605779. https://doi.org/10.1002/adfm.201605779.

[3] H. Yao, S. Sugiyama, R. Kawabata, H. Ikeda, O. Matsuoka, S. Yamamoto, N. Kitamura, Spectroscopic and AFM Studies on the Structures of Pseudoisocyanine J Aggregates at a Mica/Water Interface, J. Phys. Chem. B. 103 (1999) 4452–4456. https://doi.org/10.1021/jp990127e.

[4] F.C. Spano, The Spectral Signatures of Frenkel Polarons in H- and J-Aggregates, Acc. Chem. Res. 43 (2010) 429–439. https://doi.org/10.1021/ar900233v.

[5] F.C. Spano, C. Silva, H- and J-Aggregate Behavior in Polymeric Semiconductors, Annual Review of Physical Chemistry. 65 (2014) 477–500. https://doi.org/10.1146/annurev-physchem-040513-103639.

[6] J. Zhu, Y. Han, R. Kumar, Y. He, K. Hong, P.V. Bonnesen, B.G. Sumpter, S.C. Smith, G.S. Smith, I.N. Ivanov, C. Do, Controlling molecular ordering in solution-state conjugated polymers, Nanoscale. 7 (2015) 15134–15141. https://doi.org/10.1039/C5NR02037A.

[7] M. Baghgar, J.A. Labastide, F. Bokel, R.C. Hayward, M.D. Barnes, Effect of Polymer Chain Folding on the Transition from H- to J-Aggregate Behavior in P3HT Nanofibers, J. Phys. Chem. C. 118 (2014) 2229–2235. https://doi.org/10.1021/jp411668g.

[8] O.P. Dimitriev, D.A. Blank, C. Ganser, C. Teichert, Effect of the Polymer Chain Arrangement on Exciton and Polaron Dynamics in P3HT and P3HT:PCBM Films, J. Phys. Chem. C. 122 (2018) 17096–17109. https://doi.org/10.1021/acs.jpcc.8b05155.

[9] S. Agbolaghi, S. Zenoozi, A comprehensive review on poly(3-alkylthiophene)-based crystalline structures, protocols and electronic applications, Organic Electronics. 51 (2017) 362–403. https://doi.org/10.1016/j.orgel.2017.09.038.

[10] Y. Deng, X. Feng, D. Yang, C. Yi, X. Qiu, Pi-Pi Stacking of the aromatic groups in lignosulfonates, BioResources. 7 (2012) 1145–1156. https://doi.org/10.15376/biores.7.1.1145-1156.

[11] S.E. Domínguez, M. Cangiotti, A. Fattori, T. Ääritalo, P. Damlin, M.F. Ottaviani, C. Kvarnström, Effect of Spacer Length and Solvent on the Concentration-Driven Aggregation of Cationic Hydrogen-Bonding Donor Polythiophenes, Langmuir. 34 (2018) 7364–7378. https://doi.org/10.1021/acs.langmuir.8b00808.
[12] Y. Wang, R. Wang, Y. Imai, N. Hara, X. Wan, T. Nakano, π-Stacked and unstacked aggregate formation of 3,3'-diethylthiatricarbocyanine iodide, a near-infrared dye, New J. Chem. 42 (2018) 14713–14716. https://doi.org/10.1039/C8NJ02851F.
[13] H. Yao, Y. Morita, K. Kimura, Effect of organic solvents on J aggregation of pseudoisocyanine dye at mica/water interfaces: Morphological transition from three-dimension to two-dimension, Journal of Colloid and Interface Science. 318 (2008) 116–123. https://doi.org/10.1016/j.jcis.2007.10.003.
[14] S.S. Ono, H. Yao, O. Matsuoka, R. Kawabata, N. Kitamura, S. Yamamoto, Anisotropic Growth of J Aggregates of Pseudoisocyanine Dye at a Mica/Solution Interface Revealed by AFM and Polarization Absorption Measurements, J. Phys. Chem. B. 103 (1999) 6909–6912. https://doi.org/10.1021/jp990735u.
[15] S.S. Ono, S. Yamamoto, H. Yao, O. Matsuoka, N. Kitamura, Morphological control of the supramolecular pseudoisocyanine J-aggregates by the functions of a mica/solution interface, Applied Surface Science. 177 (2001) 189–196. https://doi.org/10.1016/S0169-4332(01)00234-3.
[16] H. Yao, Z. Ou, Y. Morita, K. Kimura, Dynamic morphology of mesoscopic pseudoisocyanine J aggregates on mica induced by humidity treatments, Colloids and Surfaces A: Physicochemical and Engineering Aspects. 236 (2004) 31–37. https://doi.org/10.1016/j.colsurfa.2004.01.022.
[17] O.J. Rojas, Adsorption of Polyelectrolytes on Mica, Encyclopedia of Surface and Colloid Science. (2002). https://doi.org/10.1081/E-ESCS3-120000912.
[18] A. Gutacker, N. Koenen, U. Scherf, S. Adamczyk, J. Pina, S.M. Fonseca, A.J.M. Valente, R.C. Evans, J. Seixas de Melo, H.D. Burrows, M. Knaapila, Cationic fluorene-thiophene diblock copolymers: Aggregation behaviour in methanol/water and its relation to thin film structures, Polymer. 51 (2010) 1898–1903. https://doi.org/10.1016/j.polymer.2010.03.010.
[19] J.E. Houston, S. Richeter, S. Clément, R.C. Evans, Molecular design of interfacial layers based on conjugated polythiophenes for polymer and hybrid solar cells, Polymer International. 66 (2017) 1333–1348. https://doi.org/10.1002/pi.5397.
[20] R. Singh, S.R. Suranagi, J. Lee, H. Lee, M. Kim, K. Cho, Unraveling the efficiency-limiting morphological issues of the perylene diimide-based non-fullerene organic solar cells, Scientific Reports. 8 (2018) 2849. https://doi.org/10.1038/s41598-018-21162-x.
[21] N.D. Treat, M.A. Brady, G. Smith, M.F. Toney, E.J. Kramer, C.J. Hawker, M.L. Chabinyc, Interdiffusion of PCBM and P3HT Reveals Miscibility in a Photovoltaically Active Blend, Advanced Energy Materials. 1 (2011) 82–89. https://doi.org/10.1002/aenm.201000023.
[22] M. Kim, J. Lee, S.B. Jo, D.H. Sin, H. Ko, H. Lee, S.G. Lee, K. Cho, Critical factors governing vertical phase separation in polymer–PCBM blend films for organic solar cells, J. Mater. Chem. A. 4 (2016) 15522–15535. https://doi.org/10.1039/C6TA06508B.
[23] S. Kouijzer, J.J. Michels, M. van den Berg, V.S. Gevaerts, M. Turbiez, M.M. Wienk, R.A.J. Janssen, Predicting Morphologies of Solution Processed Polymer:Fullerene Blends, J. Am. Chem. Soc. 135 (2013) 12057–12067. https://doi.org/10.1021/ja405493j.
[24] S.R. Dupont, E. Voroshazi, P. Heremans, R.H. Dauskardt, Adhesion properties of inverted polymer solarcells: Processing and film structure parameters, Organic Electronics. 14 (2013) 1262–1270. https://doi.org/10.1016/j.orgel.2013.02.022.
[25] J.R. Manders, S.-W. Tsang, M.J. Hartel, T.-H. Lai, S. Chen, C.M. Amb, J.R. Reynolds, F. So, Solution-Processed Nickel Oxide Hole Transport Layers in High Efficiency Polymer Photovoltaic Cells, Advanced Functional Materials. 23 (2013) 2993–3001. https://doi.org/10.1002/adfm.201202269.
[26] I. Lee, J. Noh, J.-Y. Lee, T.-S. Kim, Cooptimization of Adhesion and Power Conversion Efficiency of Organic Solar Cells by Controlling Surface Energy of Buffer Layers, ACS Appl. Mater. Interfaces. 9 (2017) 37395–37401. https://doi.org/10.1021/acsami.7b10398.
[27] W. Lee, J.H. Seo, H.Y. Woo, Conjugated polyelectrolytes: A new class of semiconducting material for organic electronic devices, Polymer (United Kingdom). 54 (2013) 5104–5121. https://doi.org/10.1016/j.polymer.2013.07.015.

[28] M.J. Higgins, G.G. Wallace, Surface and Biomolecular Forces of Conducting Polymers, Polymer Reviews. 53 (2013) 506–526. https://doi.org/10.1080/15583724.2013.813856.
[29] M.J. Tapia, M. Montserín, A.J.M. Valente, H.D. Burrows, R. Mallavia, Binding of polynucleotides to conjugated polyelectrolytes and its applications in sensing, Advances in Colloid and Interface Science. 158 (2010) 94–107. https://doi.org/10.1016/j.cis.2009.09.001.
[30] E.E. Dormidontova, Role of Competitive PEO−Water and Water−Water Hydrogen Bonding in Aqueous Solution PEO Behavior, Macromolecules. 35 (2002) 987–1001. https://doi.org/10.1021/ma010804e.
[31] T.-Q. Nguyen, V. Doan, B.J. Schwartz, Conjugated polymer aggregates in solution: Control of interchain interactions, J. Chem. Phys. 110 (1999) 4068–4078. https://doi.org/10.1063/1.478288.
[32] C. McDowell, M. Abdelsamie, M.F. Toney, G.C. Bazan, Solvent Additives: Key Morphology-Directing Agents for Solution-Processed Organic Solar Cells, Advanced Materials. 30 (2018). https://doi.org/10.1002/adma.201707114.
[33] S.E. Domínguez, A. Vuolle, M. Cangiotti, A. Fattori, T. Ääritalo, P. Damlin, M.F. Ottaviani, C. Kvarnström, Cationic Imidazolium Polythiophenes: Effects of Imidazolium-Methylation on Solution Concentration-Driven Aggregation and Surface Free Energy of Films Processed from Solvents with Different Polarity, Langmuir. 36 (2020) 2278–2290. https://doi.org/10.1021/acs.langmuir.9b03095.
[34] H.S. Lee, D.H. Kim, J.H. Cho, M. Hwang, Y. Jang, K. Cho, Effect of the Phase States of Self-Assembled Monolayers on Pentacene Growth and Thin-Film Transistor Characteristics, J. Am. Chem. Soc. 130 (2008) 10556–10564. https://doi.org/10.1021/ja800142t.
[35] J. Kesters, S. Govaerts, G. Pirotte, J. Drijkoningen, M. Chevrier, N. Van Den Brande, X. Liu, M. Fahlman, B. Van Mele, L. Lutsen, D. Vanderzande, J. Manca, S. Clément, E. Von Hauff, W. Maes, High-Permittivity Conjugated Polyelectrolyte Interlayers for High-Performance Bulk Heterojunction Organic Solar Cells, ACS Applied Materials and Interfaces. 8 (2016) 6309–6314. https://doi.org/10.1021/acsami.6b00242.
[36] S.E. Domínguez, M. Meriläinen, T. Ääritalo, P. Damlin, C. Kvarnström, Effect of alkoxy-spacer length and solvent on diluted solutions of cationic isothiouronium polythiophenes, RSC Adv. 7 (2017) 7648–7657. https://doi.org/10.1039/C6RA21451G.
[37] P. Damlin, M. Hätönen, S.E. Domínguez, T. Ääritalo, H. Kivelä, C. Kvarnström, Study of the electrochemical and optical properties of fullerene and methano[60]fullerenediphosphonate derivatives in solution and as self-assembled structures, RSC Adv. 4 (2014) 8391–8401. https://doi.org/10.1039/C3RA46740F.
[38] K. Lukkari, M. Salomaki, A. Viinikanoja, T. Aaritalo, J. Paukkunen, N. Kocharova, J. Kankare, Polyelectrolyte Multilayers Prepared from Water-Soluble\nPoly(alkoxythiophene) Derivatives, J. Am. Chem. Soc. 123 (2001) 6083–6083. https://doi.org/10.1021/ja0043486.
[39] A. Viinikanoja, S. Areva, N. Kocharova, T. Ääritalo, M. Vuorinen, A. Savunen, J. Kankare, J. Lukkari, Structure of Self-Assembled Multilayers Prepared from Water-Soluble Polythiophenes, Langmuir. 22 (2006) 6078–6086. https://doi.org/10.1021/la060519u.
[40] M. Knaapila, R.C. Evans, V.M. Garamus, L. Almásy, N.K. Székely, A. Gutacker, U. Scherf, H.D. Burrows, Structure and “surfactochromic” properties of conjugated polyelectrolyte (CPE): surfactant complexes between a cationic polythiophene and SDS in water., Langmuir : The ACS Journal of Surfaces and Colloids. 26 (2010) 15634–15643. https://doi.org/10.1021/la102591b.
[41] M. Chayer, K. Faïd, M. Leclerc, Highly Conducting Water-Soluble Polythiophene Derivatives, Chem. Mater. 9 (1997) 2902–2905. https://doi.org/10.1021/cm970238v.
[42] H.-A. Ho, M. Boissinot, M.G. Bergeron, G. Corbeil, K. Doré, D. Boudreau, M. Leclerc, Colorimetric and Fluorometric Detection of Nucleic Acids Using Cationic Polythiophene Derivatives, Angewandte Chemie. 114 (2002) 1618–1621. https://doi.org/10.1002/1521-3757(20020503)114:9<1618::AID-ANGE1618>3.0.CO;2-2.
[43] R.D.M. Malika Jeffries-El, 9. Regioregular Polythiophenes, in: J.R.R. Terje A. Skotheim (Ed.), Handbook of Conducting Polymers Third Edition CONJUGATED POLYMERS THEORY, SYNTHESIS, PROPERTIES, AND CHARACTERIZATION, Third, CRC Press Taylor & Francis Group, 2007.
[44] K.-Y. Pu, G. Wang, B. Liu, 1. Design and Synthesis of Conjugated Polyelectrolytes, in: Conjugated Polyelectrolytes, John Wiley & Sons, Ltd, 2013: pp. 1–64. https://doi.org/10.1002/9783527655700.ch1.

[45] T. Minami, Y. Kubo, Fluorescence sensing of phytate in water using an isothiouronium-attached polythiophene, Chemistry - An Asian Journal. 5 (2010) 605–611. https://doi.org/10.1002/asia.200900444.
[46] J.G. Matisons, Silanes and Siloxanes as Coupling Agents to Glass: A Perspective, in: M.J. Owen, P.R. Dvornic (Eds.), Silicone Surface Science, Springer Netherlands, Dordrecht, 2012: pp. 281–298. https://doi.org/10.1007/978-94-007-3876-8_10.
[47] S.A. Boer, P.-X. Wang, M.J. MacLachlan, N.G. White, Open Pentiptycene Networks Assembled through Charge-Assisted Hydrogen Bonds, Crystal Growth & Design. 19 (2019) 4829–4835. https://doi.org/10.1021/acs.cgd.9b00801.
[48] J. Wu, F. Liu, H. Yang, S. Xu, Q. Xie, M. Zhang, T. Chen, G. Hu, J. Wang, Effect of specific functional groups on oil adhesion from mica substrate: Implications for low salinity effect, Journal of Industrial and Engineering Chemistry. 56 (2017) 342–349. https://doi.org/10.1016/j.jiec.2017.07.030.
[49] E. Pouryousefy, Q. Xie, A. Saeedi, Effect of multi-component ions exchange on low salinity EOR: Coupled geochemical simulation study, Petroleum. 2 (2016) 215–224. https://doi.org/10.1016/j.petlm.2016.05.004.
[50] A.-F. Li, J.-H. Wang, F. Wang, Y.-B. Jiang, Anion complexation and sensing using modified urea and thiourea-based receptors, Chemical Society Reviews. 39 (2010) 3729–3729. https://doi.org/10.1039/b926160p.
[51] E. Fan, S.A. Van Arman, S. Kincaid, A.D. Hamilton, Molecular recognition: hydrogen-bonding receptors that function in highly competitive solvents, J. Am. Chem. Soc. 115 (1993) 369–370. https://doi.org/10.1021/ja00054a066.
[52] W.-S. Yeo, J.-I. Hong, Oxoanion recognition by a thiouronium receptor, Tetrahedron Letters. 39 (1998) 8137–8140. https://doi.org/10.1016/S0040-4039(98)01806-1.
[53] D.E. Gómez, L. Fabbrizzi, M. Licchelli, E. Monzani, Urea vs. thiourea in anion recognition, Org. Biomol. Chem. 3 (2005) 1495–1500. https://doi.org/10.1039/B500123D.
[54] C. Bazzicalupi, A. Bencini, V. Lippolis, Tailoring cyclic polyamines for inorganic/organic phosphate binding, Chemical Society Reviews. 39 (2010) 3709–3709. https://doi.org/10.1039/b926161n.
[55] K.-W. Tsai, C.-C. Chueh, S.T. Williams, T.-C. Wen, A.K.Y. Jen, High-performance hole-transporting layer-free conventional perovskite/fullerene heterojunction thin-film solar cells, J. Mater. Chem. A. 3 (2015) 9128–9132. https://doi.org/10.1039/C5TA01343G.
[56] J. Bernstein, R.E. Davis, L. Shimoni, N.-L. Chang, Patterns in Hydrogen Bonding: Functionality and Graph Set Analysis in Crystals, Angewandte Chemie International Edition in English. 34 (1995) 1555–1573. https://doi.org/10.1002/anie.199515551.
[57] P.A. Hunt, C.R. Ashworth, R.P. Matthews, Hydrogen bonding in ionic liquids, Chem. Soc. Rev. 44 (2015) 1257–1288. https://doi.org/10.1039/C4CS00278D.
[58] F.E. Critchfield, J.A. Gibson Jr., J.L. Hall, Dielectric Constant for the Dioxane—Water System from 20 to 35°, Journal of the American Chemical Society. 75 (1953) 1991–1992. https://doi.org/10.1021/ja01104a506.
[59] M.R. Kris, EFFECT OF 1 , 4-DIOXANE ON THE COMPLEXATION OF LANTHANIDES WITH α -HYDROXY-ISOBUTYRATE By MARIA REBECCA KRIZ A dissertation submitted in partial fulfillment of the requirements for the degree of DOCTOR OF PHILOSOPHY Department of Chemistry DECEMBER 2010, (2010).
[60] A.F.M. Barton, CRC Handbook of Solubility Parameters and Other Cohesion Parameters, Second Edition, Second, CRC Press, 1991.
[61] H.D. Burrows, S.M. Fonseca, C.L. Silva, A.A.C.C. Pais, M.J. Tapia, S. Pradhan, U. Scherf, Aggregation of the hairy rod conjugated polyelectrolyte poly{1,4-phenylene-[9,9-bis(4-phenoxybutylsulfonate)]fluorene-2,7-diyl} in aqueous solution: an experimental and molecular modelling study, Phys Chem Chem Phys. 10 (2008) 4420–4428. https://doi.org/10.1039/b800773j.
[62] T.Q. Luong, P.K. Verma, R.K. Mitra, M. Havenith, Onset of Hydrogen Bonded Collective Network of Water in 1,4-Dioxane, J. Phys. Chem. A. 115 (2011) 14462–14469. https://doi.org/10.1021/jp204927r.
[63] T. Nakagawa, J. Hatano, Y. Matsuo, Influence of additives in bulk heterojunction solar cells using magnesium tetraethynylporphyrin with triisopropylsilyl and anthryl substituents, J. Porphyrins Phthalocyanines. 18 (2014) 735–740. https://doi.org/10.1142/S1088424614500655.

[64] S. Chen, Z. Liu, Z. Ge, Synthesis, characterization and photovoltaic properties of three new 3,4-dithienyl-substituted polythiophene derivatives, Polymer Journal. 48 (2016) 101–110. https://doi.org/10.1038/pj.2015.85.
[65] M.J. Kamlet, J.L.M. Abboud, M.H. Abraham, R.W. Taft, Linear solvation energy relationships. 23. A comprehensive collection of the solvatochromic parameters, .pi.*, .alpha., and .beta., and some methods for simplifying the generalized solvatochromic equation, J. Org. Chem. 48 (1983) 2877–2887. https://doi.org/10.1021/jo00165a018.
[66] C. Reichardt, Solvatochromic Dyes as Solvent Polarity Indicators, Chem. Rev. 94 (1994) 2319–2358. https://doi.org/10.1021/cr00032a005.
[67] C.A. Hunter, Quantifying Intermolecular Interactions: Guidelines for the Molecular Recognition Toolbox, Angewandte Chemie International Edition. 43 (2004) 5310–5324. https://doi.org/10.1002/anie.200301739.
[68] V. Belandria, A.H. Mohammadi, D. Richon, Volumetric properties of the (tetrahydrofuran + water) and (tetra-n-butyl ammonium bromide + water) systems: Experimental measurements and correlations, Journal of Chemical Thermodynamics. 41 (2009) 1382–1386. https://doi.org/10.1016/j.jct.2009.06.014.
[69] E.R. Smith, M. Wojciechowski, BOILING-POINT-COMPOSITION DIAGRAM OF THE SYSTEM DIOXANE-WATER, Journal of Research of the N.Ational Bureau of Standards. 18 (1937).
[70] J. Nayak, M. Aralaguppi, B.V. Naidu, T. Aminabhavi, Thermodynamic Properties of Water + Tetrahydrofuran and Water + 1 , 4-Dioxane Mixtures at (303 . 15 , 313 . 15 , and 323 . 15) K, J. Chem. Eng. Data. 49 (2004) 468–474.
[71] F.E. Critchfield, J.A. Gibson Jr., J.L. Hall, Dielectric Constant for the Dioxane—Water System from 20 to 35°, Journal of the American Chemical Society. 75 (1953) 1991–1992. https://doi.org/10.1021/ja01104a506.
[72] L.-M. Omota, O. Iulian, F. Omota, O. Ciocirlan, DENSITIES AND DERIVED PROPERTIES OF WATER, 1,4-DIOXANE AND DIMETHYL SULFOXIDE BINARY AND TERNARY SYSTEMS AT TEMPERATURES FROM 293.15 K TO 313.15 K, Revue Roumaine de Chimie. 54 (2009) 63–73.
[73] A.F.M. Barton, CRC Handbook of Solubility Parameters and Other Cohesion Parameters, Second Edition, Second, CRC Press, 1991. https://doi.org/9780849301766 - CAT# 176.
[74] C.M. Hansen, Hansen Solubility Parameters: A User's Handbook, Second Edition, 2007.
[75] F. Menges, Spectragryph - optical spectroscopy software, Version 1.0.3, 2017, http://www.effemm2.de/spectragryph/, 2017. http://www.effemm2.de/spectragryph/.
[76] J. Kesters, S. Govaerts, G. Pirotte, J. Drijkoningen, M. Chevrier, N. Van Den Brande, X. Liu, M. Fahlman, B. Van Mele, L. Lutsen, D. Vanderzande, J. Manca, S. Clément, E. Von Hauff, W. Maes, High-Permittivity Conjugated Polyelectrolyte Interlayers for High-Performance Bulk Heterojunction Organic Solar Cells, ACS Applied Materials and Interfaces. 8 (2016) 6309–6314. https://doi.org/10.1021/acsami.6b00242.
[77] J. Schindelin, I. Arganda-Carreras, E. Frise, V. Kaynig, M. Longair, T. Pietzsch, S. Preibisch, C. Rueden, S. Saalfeld, B. Schmid, J.-Y. Tinevez, D.J. White, V. Hartenstein, K. Eliceiri, P. Tomancak, A. Cardona, Fiji: an open-source platform for biological-image analysis, Nature Methods. 9 (2012) 676–682. https://doi.org/10.1038/nmeth.2019.
[78] M.A. Model, Intensity Calibration and Shading Correction for Fluorescence Microscopes, Current Protocols in Cytometry. 37 (2006) 10.14.1-10.14.7. https://doi.org/10.1002/0471142956.cy1014s37.
[79] Z.V. Leonenko, E. Finot, D.T. Cramb, Atomic Force Microscopy to Study Interacting Forces in Phospholipid Bilayers Containing General Anesthetics, in: A.M. Dopico (Ed.), Methods in Membrane Lipids, Humana Press, Totowa, NJ, 2007: pp. 601–609. https://doi.org/10.1007/978-1-59745-519-0_40.
[80] M. Wang, S. Zou, G. Guerin, L. Shen, K. Deng, M. Jones, G.C. Walker, G.D. Scholes, M.A. Winnik, A Water-Soluble pH-Responsive Molecular Brush of Poly(N,N-dimethylaminoethyl methacrylate) Grafted Polythiophene, Macromolecules. 41 (2008) 6993–7002. https://doi.org/10.1021/ma800777m.
[81] D. Nečas, P. Klapetek, Gwyddion: an open-source software for SPM data analysis, Centr.Eur.j.Phys. 10 (2012) 181–188. https://doi.org/10.2478/s11534-011-0096-2.

[82] J.K. Keum, K. Xiao, I.N. Ivanov, K. Hong, J.F. Browning, G.S. Smith, M. Shao, K.C. Littrell, A.J. Rondinone, E. Andrew Payzant, J. Chen, D.K. Hensley, Solvent quality-induced nucleation and growth of parallelepiped nanorods in dilute poly(3-hexylthiophene) (P3HT) solution and the impact on the crystalline morphology of solution-cast thin film, CrystEngComm. 15 (2013) 1114–1124. https://doi.org/10.1039/C2CE26666K.
[83] R.F. Cossiello, L. Akcelrud, T.D.Z. Atvars, Solvent and molecular weight effects on fluorescence emission of MEH-PPV, Journal of the Brazilian Chemical Society. 16 (2005) 74–86. https://doi.org/10.1590/S0103-50532005000100012.
[84] Z. Hu, A.P. Willard, R.J. Ono, C.W. Bielawski, P.J. Rossky, D.A. Vanden Bout, An insight into non-emissive excited states in conjugated polymers, Nature Communications. 6 (2015) 1–9. https://doi.org/10.1038/ncomms9246.
[85] A. Åslund, Designing thiophene-based fluorescent probes for the study of neurodegenerative protein aggregation diseases From test tube to in vivo experiments, 2009.
[86] S.K. Saikin, A. Eisfeld, S. Valleau, A. Aspuru-Guzik, Photonics meets excitonics: Natural and artificial molecular aggregates, Nanophotonics. 2 (2013) 21–38. https://doi.org/10.1515/nanoph-2012-0025.
[87] T.C. Werner, D.M. Hercules, Fluorescence of 9-anthroic acid and its esters. Environmental effects on excited-state behavior, J. Phys. Chem. 73 (1969) 2005–2011. https://doi.org/10.1021/j100726a060.
[88] T.C. Werner, R.M. Hoffman, Relation between an excited state geometry change and the solvent dependence of 9-methyl anthroate fluorescence, J. Phys. Chem. 77 (1973) 1611–1615. https://doi.org/10.1021/j100632a003.
[89] B.F. Hermenegildo, G. Pereira, A.S. Abreu, E.M.S. Castanheira, P.M.T. Ferreira, M.J.R.P. Queiroz, Phenanthrenyl-indole as a fluorescent probe for peptides and lipid membranes, Journal of Photochemistry and Photobiology A: Chemistry. 221 (2011) 47–57. https://doi.org/10.1016/j.jphotochem.2011.04.022.
[90] W.-N. He, J.-T. Xu, Crystallization assisted self-assembly of semicrystalline block copolymers, Progress in Polymer Science. 37 (2012) 1350–1400. https://doi.org/10.1016/j.progpolymsci.2012.05.002.
[91] T.A. Witten, L.M. Sander, Diffusion-Limited Aggregation, a Kinetic Critical Phenomenon, Phys. Rev. Lett. 47 (1981) 1400–1403. https://doi.org/10.1103/PhysRevLett.47.1400.
[92] T.A. Witten, L.M. Sander, Diffusion-limited aggregation, Phys. Rev. B. 27 (1983) 5686–5697. https://doi.org/10.1103/PhysRevB.27.5686.
[93] K.N. Liou, Y. Takano, P. Yang, Light absorption and scattering by aggregates: Application to black carbon and snow grains, Journal of Quantitative Spectroscopy and Radiative Transfer. 112 (2011) 1581–1594. https://doi.org/10.1016/j.jqsrt.2011.03.007.
[94] I.R. Nogueira, S.G. Alves, S.C. Ferreira, Scaling laws in the diffusion limited aggregation of persistent random walkers, Physica A: Statistical Mechanics and Its Applications. 390 (2011) 4087–4094. https://doi.org/10.1016/j.physa.2011.06.077.
[95] L. Tumbek, A. Winkler, Attachment limited versus diffusion limited nucleation of organic molecules: Hexaphenyl on sputter-modified mica, Surface Science. 606 (2012) L55–L58. https://doi.org/10.1016/j.susc.2012.03.018.
[96] A. Winkler, L. Tumbek, Nucleation of Organic Molecules via a Hot Precursor State: Pentacene on Amorphous Mica, J. Phys. Chem. Lett. 4 (2013) 4080–4084. https://doi.org/10.1021/jz402301v.
[97] D. Rymuszka, K. Terpiłowski, L. Hołysz, Influence of Volume Drop on Surface Free Energy of Glass, Annales UMCS, Chemia. 68 (2014) 121–132. https://doi.org/10.2478/umcschem-2013-0010.
[98] B. Jańczuk, I. Choma, A.L. Dawidowicz, A. Kliszcz, T. Białopiotrowicz, Correlation between the surface free energy of modified and non-modified glasses with controlled porosity and their sorption properties, Chromatographia. 30 (1990) 382–387. https://doi.org/10.1007/BF02328502.
[99] R. Yan, Y. Wang, T.V. Duncan, Y.C. Shieh, Effect of polymer and glass physicochemical properties on MS2 recovery from food contact surfaces, Food Microbiology. 87 (2020) 103354. https://doi.org/10.1016/j.fm.2019.103354.
[100] M.J. Liu, K. Tzou, R.V. Gregory, Influence of the doping conditions on the surface energies of conducting polymers, Synthetic Metals. 63 (1994) 67–71. https://doi.org/10.1016/0379-6779(94)90251-8.

[101] Y.-T. Tsai, C.-H. Choi, N. Gao, E.-H. Yang, Tunable Wetting Mechanism of Polypyrrole Surfaces and Low-Voltage Droplet Manipulation via Redox, Langmuir. 27 (2011) 4249–4256. https://doi.org/10.1021/la104403w.